

NACA TM 1428

816L

TECH LIBRARY KAFB, NM
0144579

NATIONAL ADVISORY COMMITTEE FOR AERONAUTICS

TECHNICAL MEMORANDUM 1428

EFFECT OF FATIGUE CRACK ON STATIC STRENGTH:

2014-T6, 2024-T4, 6061-T6, 7075-T6

OPEN-HOLE MONOBLOC SPECIMENS

By Glenn E. Nordmark and Ian D. Eaton

Aluminum Company of America



Washington

May 1957

AFMDC
TECHNICAL LIBRARY
APR 2007



NATIONAL ADVISORY COMMITTEE FOR AERONAUTICS

TECHNICAL MEMORANDUM 1428

EFFECT OF FATIGUE CRACK ON STATIC STRENGTH:

2014-T6, 2024-T4, 6061-T6, 7075-T6

OPEN-HOLE MONOBLOC SPECIMENS*

By Glenn E. Nordmark and Ian D. Eaton

SYNOPSIS

Static tensile test results are presented for specimens of 2014-T6, 2024-T4, 6061-T6, and 7075-T6 aluminum alloy containing fatigue cracks. The results are found to be in good agreement with the results reported for similar tests from other sources.

The results indicate that the presence of a fatigue crack reduced the static strength, in all cases, by an amount larger than the corresponding reduction in net area; the 6061-T6 alloy specimens were least susceptible to the crack and the 7075-T6 alloy specimens most susceptible. It is indicated that a 7075-T6 specimen may develop as little as one-third of the expected static tensile strength when the fatigue crack has consumed only one-fourth of the original area.

It was found that the static strength was substantially higher for specimens which had stop holes drilled at the end of the fatigue crack.

I. Introduction

In fatigue testing, failure is generally considered to have occurred when a visible crack initiates in the member being tested. In the design of a structure, however, it is important to know not only the number of loadings at which a crack will probably occur when a member is subjected to a certain stress cycle but also the likelihood of a resulting failure of the entire structure. Some aspects of these problems are being studied at Alcoa Research Laboratories in concurrent investigations of the rate of propagation and methods of stopping fatigue cracks. In addition, it is necessary to determine the effect of an existing fatigue crack on the static and impact strength of the member; i.e., will the decrease in strength be merely proportional to the reduction in the net section, or

*Unedited by the NACA (the Committee takes no responsibility for the correctness of the author's statements).

is the material notch sensitive so that a disproportionately large decrease in the static strength will result from the fatigue crack?

II. Object

The object of this investigation was to determine the effect of an existing fatigue crack on the static tensile properties of the following aluminum alloys: 2014-T6, 2024-T4, 6061-T6, and 7075-T6.

III. Material

From the tensile properties listed in table I, it can be seen that the tensile properties of the 1-inch by 7.5-inch aluminum-alloy rolled rectangular bars used in this investigation meet the applicable guaranteed minimum requirements as given in table 4d of reference 1.*

IV. Test Specimens

The details of the open-hole monobloc specimens used in this investigation are illustrated in figure 1. The tests of each alloy included one specimen which had not been loaded previously; all other specimens had fatigue cracks emanating from one or both sides of the central open hole as a result of having been previously subjected to cyclic tensile loadings in Templin Structural Fatigue Testing Machines described in reference 2. The fatigue tests were performed at a zero stress ratio,** the maximum net-section stress in each cycle being about 20 ksi for all the 2014-T6 and 2024-T4 specimens, 14 ksi for all the 6061-T6 specimens, and 13, 20, and 23 ksi, respectively, for the three 7075-T6 specimens. Thus, cracks were produced in the individual 2014-T6, 2024-T4, and 6061-T6 specimens using approximately the same loadings for all the specimens of each alloy, whereas the stress level differed for each 7075-T6 specimen tested. One specimen of each alloy had a 1/4-inch diameter hole drilled through the plate at the end of the fatigue crack in order that the effect of stop holes could be determined. The length of the fatigue cracks, recorded in table III, was determined by careful visual examination before the stop hole, if any, was drilled.

V. Procedure

The specimens were loaded in static tension in an Amsler Universal Testing Machine*** of the hydraulic type having multiple load ranges and

* References are listed at the end of the text.

** Stress ratio is the ratio of the minimum to the maximum stress in the cycle.

***Type 150SZBDA, Serial No. 5254. Periodic calibration of this machine indicates that the error in load readings is less than 1 percent throughout the upper 90 percent of the load range used.

a maximum capacity of 300 kips. The loading arrangement is shown in figure 2. At regular intervals of loading, the deformation in an 8-inch gage length was determined from dial gage measurements on each edge of the specimen. The test was continued to complete separation of the plate.

VI. Results

Load-deformation curves for the individual specimens of 2014-T6, 2024-T4, 6061-T6, and 7075-T6 aluminum alloys are presented in figures 3 through 6. From a comparison of the data for uncracked specimens with those for specimens containing fatigue cracks, it is evident that the cracks cause a large reduction in ductility, as measured by the total deformation, as well as a reduction in static ultimate load. For each alloy there was a general tendency for the ductility to be less for the specimens with the longer cracks. However, as might be expected, the specimens with stop holes exhibited greater deformation than the comparable specimen without the holes.

The static tensile strengths of the open-hole monobloc specimens which had not been subjected to fatigue loading are listed in table II. The loss of 11 percent in strength of the 2024-T4 specimen, due to the open hole, is in agreement with test results described in reference 3 where a single open hole in 2024-T3 sheet specimens caused a reduction of about 12 percent in the net-area tensile strength when the diameter of the hole was about 10 percent of the width of the specimen.

The tensile strengths of the uncracked specimens are compared with those of the cracked specimens in table III by use of the relative strength.* One or more specimens in each alloy were tested with a single fatigue crack of about 1-inch length; the relative strengths of the specimens without a circular stop hole are found to be:

6061-T6	79 percent
2024-T4	66 percent
2014-T6	57 percent
7075-T6	48 percent

Undoubtedly, the load is applied somewhat eccentrically to those specimens having a single crack. However, it may be seen that the two 6061-T6 specimens, 2162 and 2164, having a total crack length of about 1 inch had comparable static tensile strengths although the one had two cracks and the other one. Thus, it appears that the number of cracks did not affect the results substantially.

*Relative strength is the ratio of the strength of a cracked specimen divided by the strength of the uncracked specimen.

The relationship between the relative static strength and net area of the specimens is plotted in figure 7. The dashed line represents the case in which the percentage loss in strength is equal to the percentage loss in area. It is evident that the loss in strength was greater, in every case, than the loss in area. Although the stop hole reduced the net area, the resultant reduction of the stress concentration was obviously sufficient to more than compensate for the additional loss in area; the static strength of the specimen with stop holes, indicated by shaded symbols in figure 7, was, for each alloy, substantially above the trend of results of the specimens without stop holes.

For the specimens not having stop holes, the effect of the length of the fatigue crack on the load-carrying capacity of the specimen is shown in figure 8. These data indicate that, with a total crack length of about $1\frac{3}{4}$ inches, specimens of all four alloys have approximately the same load-carrying capacity. As no data were obtained for specimens having a total crack length greater than $1\frac{3}{4}$ inches, it is not known whether the ultimate load would vary with the alloy for specimens having longer cracks.

The effect of the length of crack can also be investigated by comparing the static-strength reduction factors listed in table III and plotted in figure 9 for the specimens without stop holes. It can be seen that the factors increase with the length of the crack. Further, the lowest curve is for alloy 6061-T6 and the curves are progressively higher for alloys 2024-T4, 2014-T6, and 7075-T6; i.e., in the same order found for the specimens with a single 1-inch-long crack and, it might be pointed out, in the inverse order of the ultimate strengths of the materials.

Data obtained from similar tests in which fatigue cracks were initiated from circular notches at the edges of narrow specimens taken from sheet and extrusions are given in reference 4. The investigation was more extensive than the one described herein in that more specimens were tested and the lengths of the fatigue cracks ranged between 1 and 60 percent of the original net width of the specimen. The curves presented therein are amply defined by test data. A few additional results of static tests of sheet specimens with simulated fatigue cracks in the center of the specimen were presented in reference 5. The results of the investigation described herein are compared with appropriate results from the cited references in figures 10 through 12. The results from the three sources appear to be in general agreement. It is to be expected that the relative static strengths of cracked specimens would be no greater than the values indicated by the dashed lines, representing the case where the relative strength is equal to the ratio of the net area, after cracking, to the original area; it can be seen that a 6061-T4 specimen with a simulated fatigue crack was the only specimen which had a strength greater than the maximum expected from the net area.

The results of static tests of two double-shear, bolted joints having fatigue cracks originating from the bolt holes are included in reference 6. It can be seen in figures 10 and 11 that the results of these joints are in good agreement with the data obtained from the open-hole and notched specimens.

VII. Conclusions

From the foregoing data and discussion of results of static tensile tests of specimens containing fatigue cracks, the following conclusions appear warranted:

1. Specimens with a single open hole of 2014-T6, 6061-T6, and 7075-T6 developed the ultimate strength of the materials across the net section of the specimen; whereas the 2024-T4 specimen had an 11-percent loss in net-section ultimate strength. A similar drop in strength has been reported in reference 3.
2. Specimens with a fatigue crack, or cracks, lose much of the ductility evidenced in tests of uncracked specimens.
3. The presence of fatigue cracks in specimens of 2014-T6, 2024-T4, 6061-T6, and 7075-T6 aluminum alloys reduces the static strength by an amount larger than the corresponding reduction in net area.
4. The use of stop holes at the end of the fatigue cracks resulted in increased load-carrying capacity and ductility, but, except for the specimen of alloy 6061-T6, the strength was still less than that expected from a consideration of the reduction in net area and the tensile strength of the material.
5. For the four alloys tested, the deleterious effect of the notch varied somewhat as the tensile strength of the alloy. For a single 1-inch crack, the strengths, expressed as a percentage of that of an uncracked specimen of the same alloy (relative strengths), were:

6061-T6	79
2024-T4	66
2014-T6	57
7075-T6	48

These factors were determined by comparison with the strengths of open-hole monobloc specimens. If the comparison is made on the basis of ultimate strength of the material, in order to eliminate any notch effect of the hole in the uncracked specimen, the value for the 2024-T4 specimen is reduced to 58, and that of the 2014-T6 specimen to 55; whereas the factors for the specimens of the other two alloys remain the same.

6. These data indicate that, with a total crack length of about $1\frac{3}{4}$ inches, specimens of all four alloys have approximately the same load-carrying capacity.

7. The results of the tests made at the Alcoa Research Laboratories are in general agreement with those reported by Langley Field and Lockheed Aircraft Company in references 4 and 5. Further, it was found that the data were in good agreement with the results reported in reference 6 for two tests of bolted joints.

REFERENCES

1. Anon.: Alcoa Structural Handbook, 1955. Aluminum Company of America, Pittsburgh, Pennsylvania.
2. Templin, R. L.: Fatigue Machines for Testing Structural Units. Proceedings ASTM, vol. 39, 1939, p. 711.
3. Hill, H. N., and Barker, R. S.: Effect of Open Circular Holes on Tensile Strength and Elongation of Sheet Specimens of Some Aluminum Alloys. NACA Technical Note 1974.
4. Illg, Walter, and Hardrath, Herbert F.: Some Observations on Loss of Static Strength Due to Fatigue Cracks. NACA Research Memorandum L55D15a, May 1955.
5. McBrearty, J. F.: Fatigue and Fail Safe Airframe Design. Presented at SAE Golden Anniversary Meeting, Los Angeles, California, October 1955. (SAE Preprint No. 610.)
6. Hartmann, E. C., Holt, Marshall, and Eaton, I. D.: Additional Static and Fatigue Tests of High-Strength Aluminum Alloy Bolted Joints. NACA Technical Note 3269.

TABLE I

TENSILE PROPERTIES OF 1- BY $7\frac{1}{2}$ - INCH ROLLED RECTANGULAR BAR*

Alloy and temper	Specimen no.	M.T. number	Tensile strength, ksi	Yield strength,** ksi	Elongation in 2-in., percent
2014-T6	146189	120753-D	69.8	63.4	11.0
	146369		67.3	60.5	11.0
			Avg. 68.6	62.0	11.0
	MINIMUM GUARANTEED†		65	55	8
2024-T4	146370	120753-D	64.8	42.0	20.0
		MINIMUM GUARANTEED	62	40	14
6061-T6	146199	080554-A	43.8	41.2	16.5
	146368	120753-E	43.8	41.8	15.0
	146379	022156-A	43.2	41.0	15.5
			Avg. 43.6	41.3	15.7
	MINIMUM GUARANTEED		42	35	10
7075-T6	146371	120753-F	87.0	78.7	10.5
		MINIMUM GUARANTEED	77	66	7

* $1/2$ -inch-diameter specimen cut from longitudinal direction. See figure 8 of "Tentative Methods of Tension Testing of Metallic Materials," ASTM Designation E8-54T. 1955 Book of ASTM Standards.

**Stress at 0.2-percent offset. Templin Autographic Extensometer (500X).

†Alcoa Structural Handbook (1955). Aluminum Company of America, Pittsburgh 19, Pa.

TABLE II

SUMMARY OF STATIC TENSILE TEST RESULTS FOR OPEN-HOLE
MONOBLOC SPECIMENS WITHOUT PRIOR FATIGUE LOADING

J.O. 12-1356

Alloy and temper	Specimen no.	Tensile strength,* ksi	Relative strength,** percent
2014-T6	2196	66.8	97
2024-T4	2192	57.4	89
6061-T6	2185	44.1	100
7075-T6	2176	87.4	100

*Tensile load ÷ net area.

**Tensile strength of specimen ÷ average tensile strength of material, from table I, x100.

TABLE III
SUMMARY OF STATIC TENSILE TEST RESULTS FOR OPEN-HOLE MONOBLOC
SPECIMENS WITH AND WITHOUT PRIOR FATIGUE LOADING

J.O. 12-1356

Specimen no.	Fatigue history					Net area** percent of original	Maximum load, kips	Gross tensile strength,† ksi	Relative strength,†† percent	Net tensile strength, ^a ksi	Strength reduction factor ^b
	Maximum stress, ksi*	Number of cycles	Crack length, in.								
			Left	Right	Total						
							2014-T6				
2196	0.00	None	0.00	0.00	0.00	100	119.5	66.8	100	66.8	1.00
924	19.94	90,200	1.00	0.00	1.00	85	64.5	37.9	57	44.3	1.50
922	19.93	88,100	0.26	0.21	0.47	93	79.0	45.4	68	49.3	1.36
923 ^c	19.98	111,400	0.00	1.01	1.01	85 ^a	90.0	31.7	77	62.0	1.08
							2024-T4				
2192	0.00	None	0.00	0.00	0.00	100	98.8	37.4	100	37.4	1.00
2195	19.92	70,400	1.01	0.00	1.01	85	65.0	37.6	66	44.2	1.30
2198	22.86	88,300	1.10	0.67	1.77	74	55.5	31.7	55	42.8	1.34
2193 ^c	19.96	940,800	1.01	0.00	1.01	85 ^a	72.0	41.2	72	49.5	1.16
							6061-T6				
2185	0.00	None	0.00	0.00	0.00	100	76.0	44.1	100	44.1	1.00
2164	14.00	279,600	0.00	1.02	1.02	85	60.9	34.9	79	41.0	1.03
2169	13.96	815,100	1.45	0.00	1.45	79	55.4	31.1	71	39.7	1.11
2162	13.97	354,900	0.46	0.52	0.98	86	60.8	34.9	79	42.8	1.08
2244 ^c	13.97	3,568,400	1.19	0.00	1.19	85 ^a	61.2	35.1	80	45.9	1.00
							7075-T6				
2176	0.00	None	0.00	0.00	0.00	100	154.0	87.4	100	87.4	1.00
2206	19.98	314,200	1.04	0.00	1.04	85	75.5	41.8	48	49.3	1.77
2184	22.46	70,200	0.79	1.02	1.81	74	54.6	30.8	35	41.8	2.10
2208 ^c	12.93	3,261,400	0.84	0.00	0.84	85 ^c	113.7	64.8	74	76.5	1.14

* Stress ratio = $\frac{\text{Minimum stress}}{\text{Maximum stress}} = 0.$

** Net area = Original area minus area of cracks and stoppage holes, if any.

† Gross tensile strength = Load ÷ Area before crack.

†† Relative strength = $\frac{\text{Strength of cracked specimen}}{\text{Strength of uncracked specimen}} \times 100.$

^a Net tensile strength = Load ÷ Area after crack.

^b Strength reduction factor = $\frac{\text{Net tensile strength of uncracked specimen}}{\text{Net tensile strength of cracked specimen}}.$

^c 1/4-inch stop hole drilled through plate at end of crack.

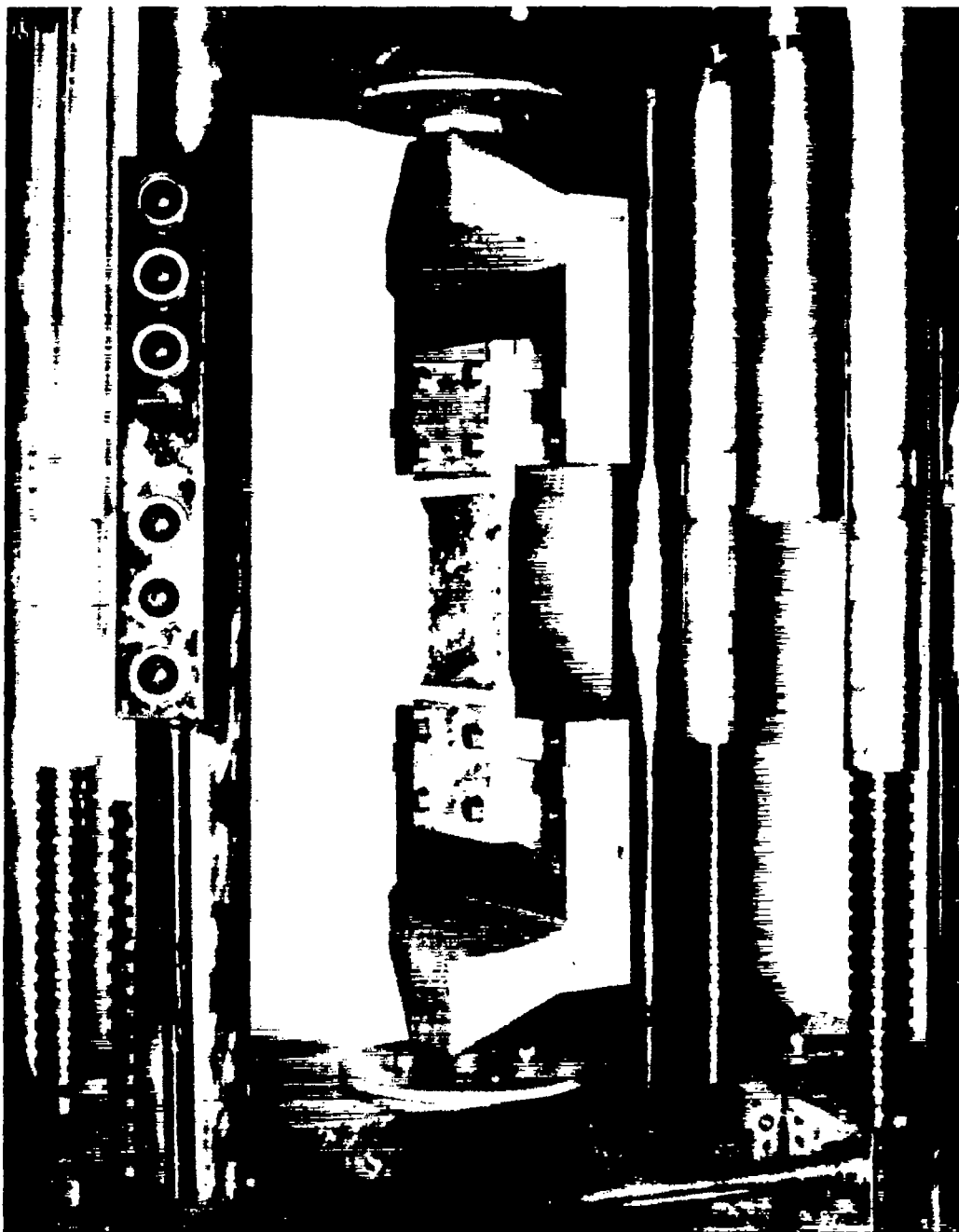
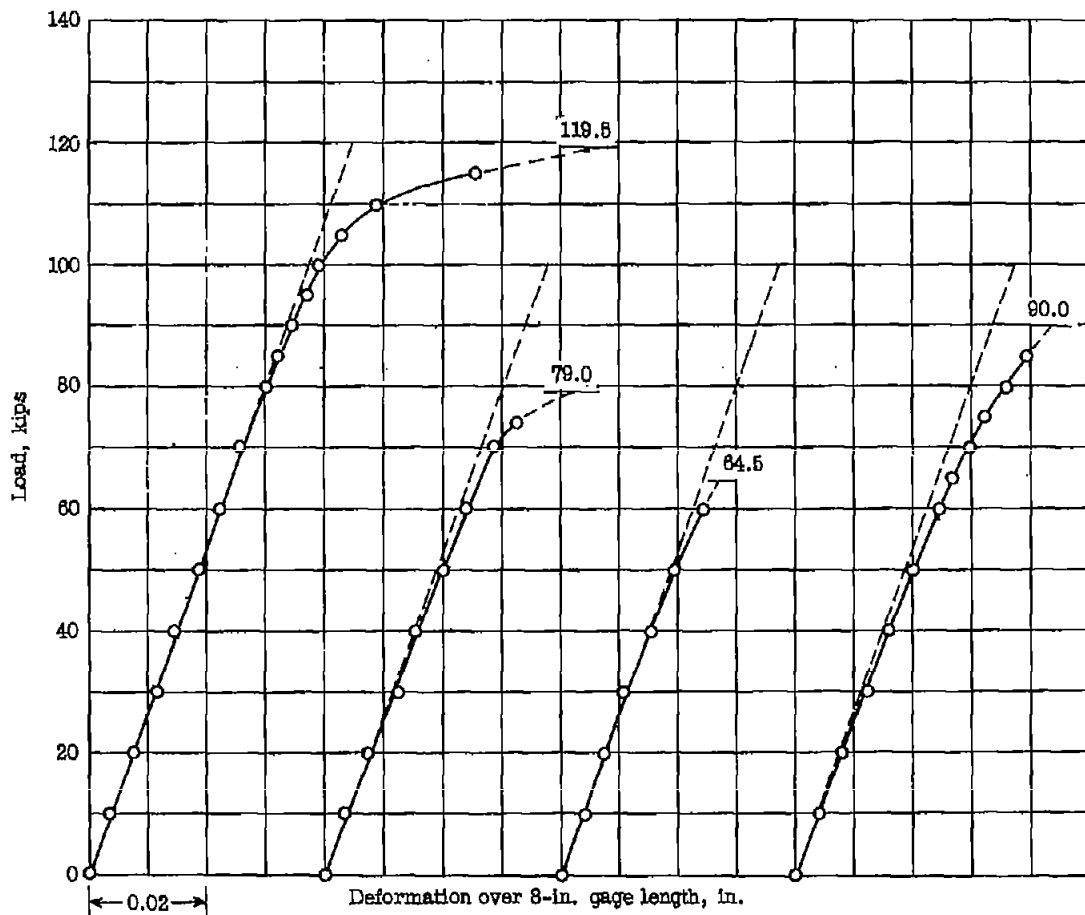
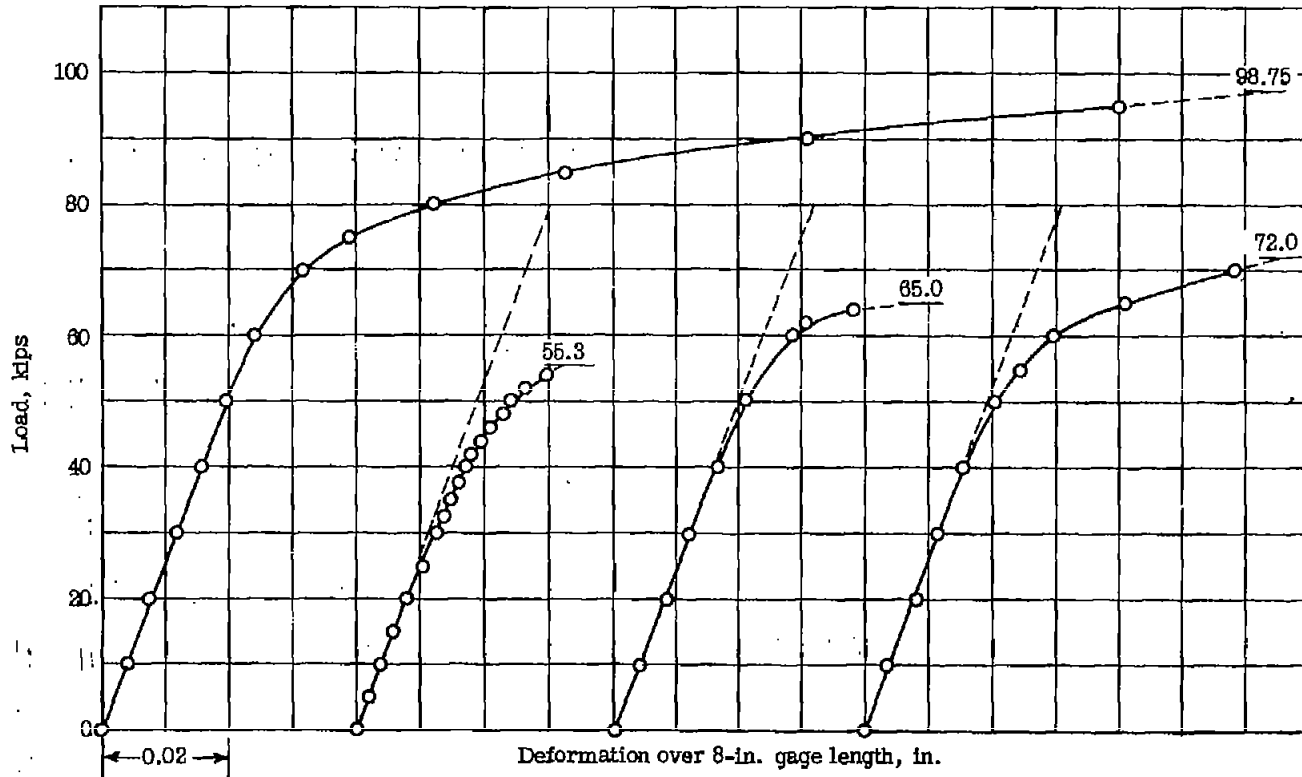


Figure 2.- Static test fixtures designed by Mr. R. L. Templin. These fixtures are equipped with spherically seated tension bolts. (Specimen shown was used in another investigation.)



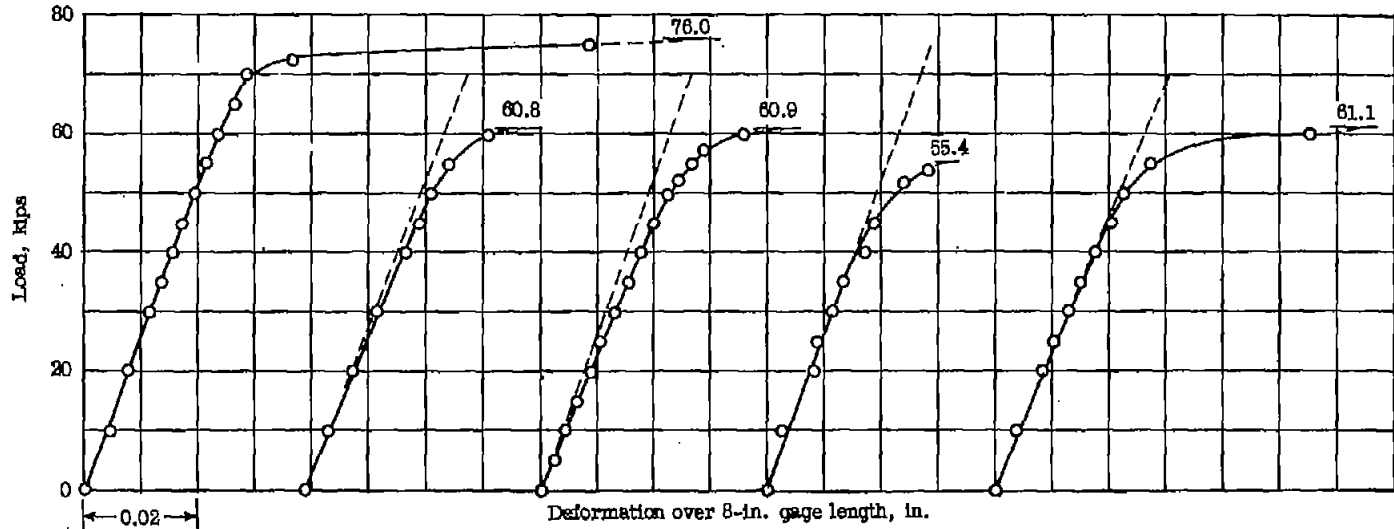
Specimen No.	2196	922	924	923
Number of cracks	0	2	1	1 (Stop hole)
Total length of cracks, in.	0	0.47	1.00	1.01

Figure 3.- Load-deformation curves for type GX specimens (with and without fatigue cracks). 2014-T6.



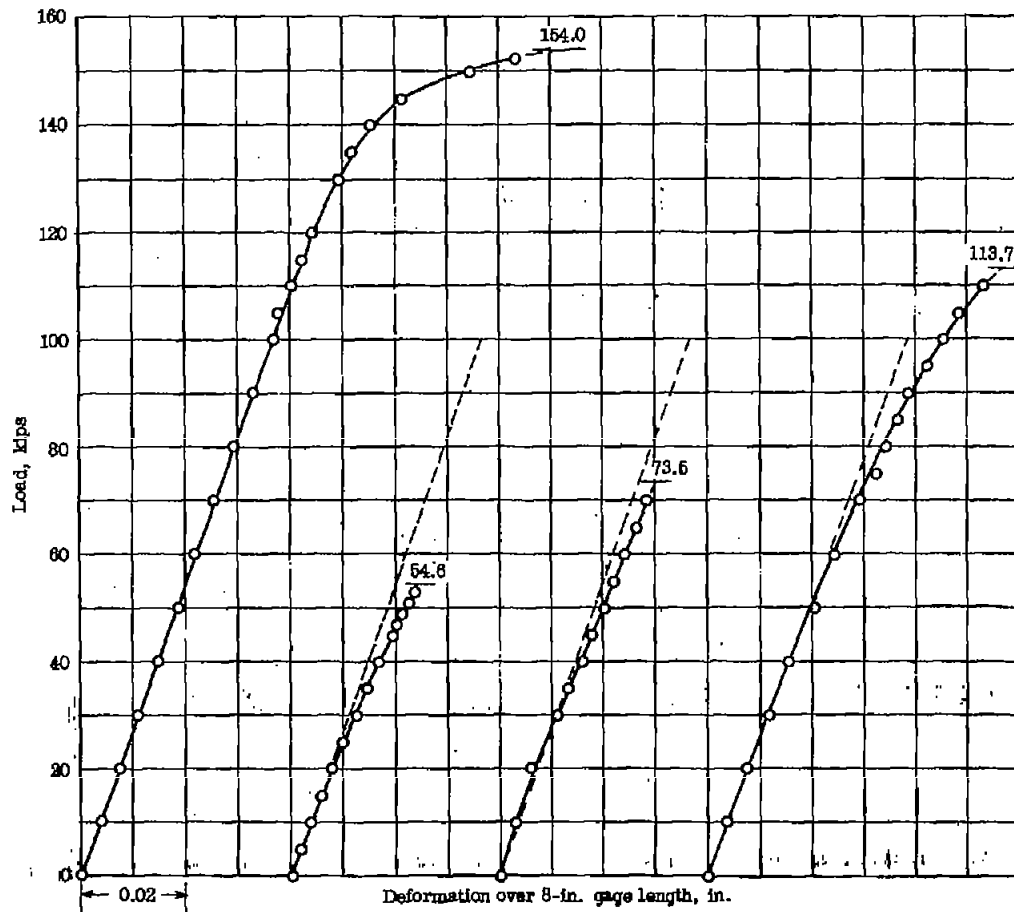
Specimen No.	2192	2198	2195	2193
Number of cracks	0	2	1	1 (Stop hole)
Total length of cracks, in.	0	1.77	1.01	0.98

Figure 4.- Load-deformation curves for type GX specimens (with and without fatigue cracks). 2024-T4.



Specimen No.	2185	2182	2184	2189	2444
Number of cracks	0	2	1	1	1 (Stop hole)
Total length of cracks, in.	0	0.98	1.02	1.45	1.19

Figure 5.- Load-deformation curves for type GX specimens (with and without fatigue cracks). 6061-T6.



Specimen No.	2176	2184	2206	2208
Number of cracks	0	2	1	1 (Stop hole)
Total length of cracks, in.	0	1.81	1.04	0.84

Figure 6.- Load-deformation curves for type GX specimens (with and without fatigue cracks). 7075-T6.

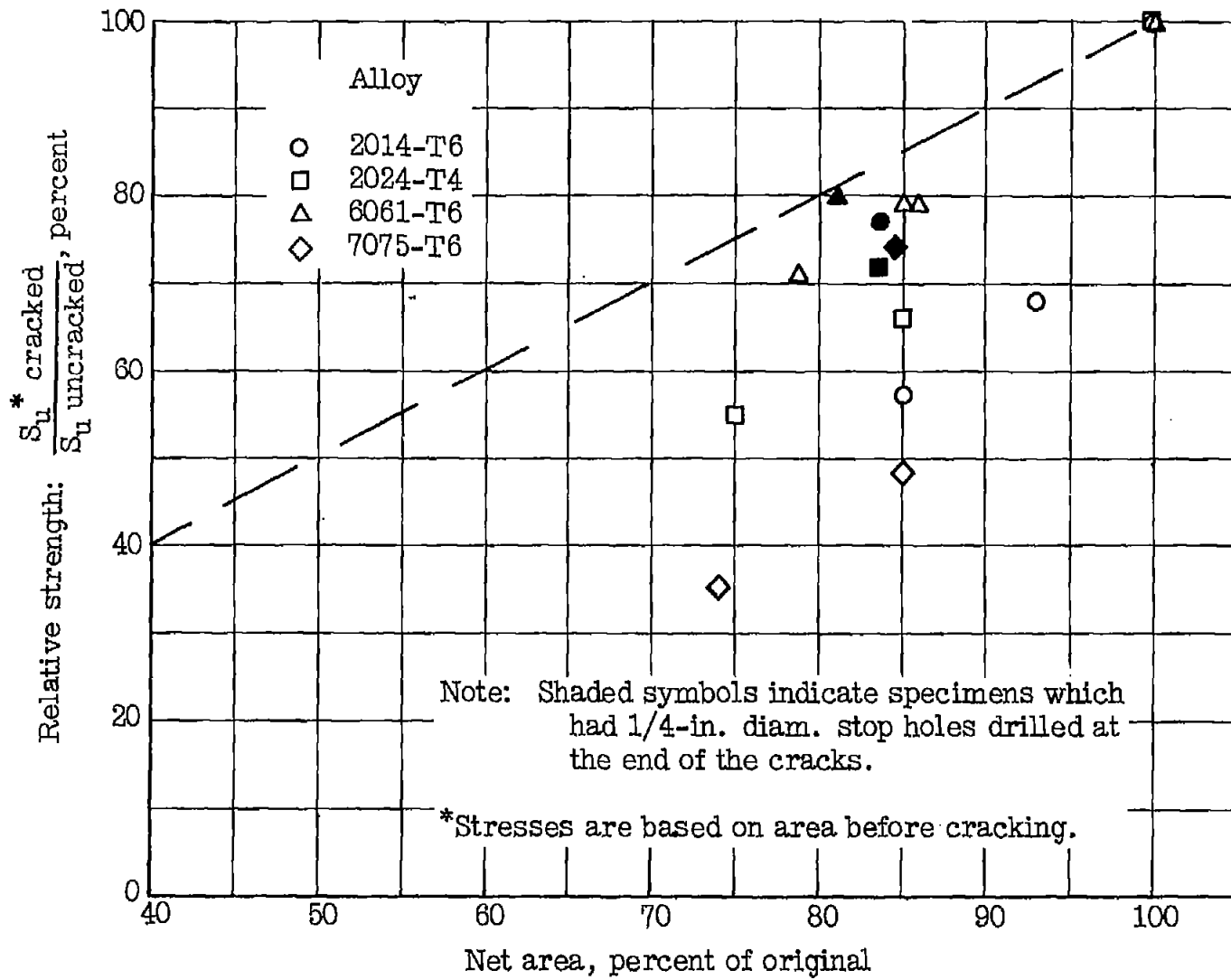


Figure 7.- Effect of fatigue crack on static strength of aluminum alloys.

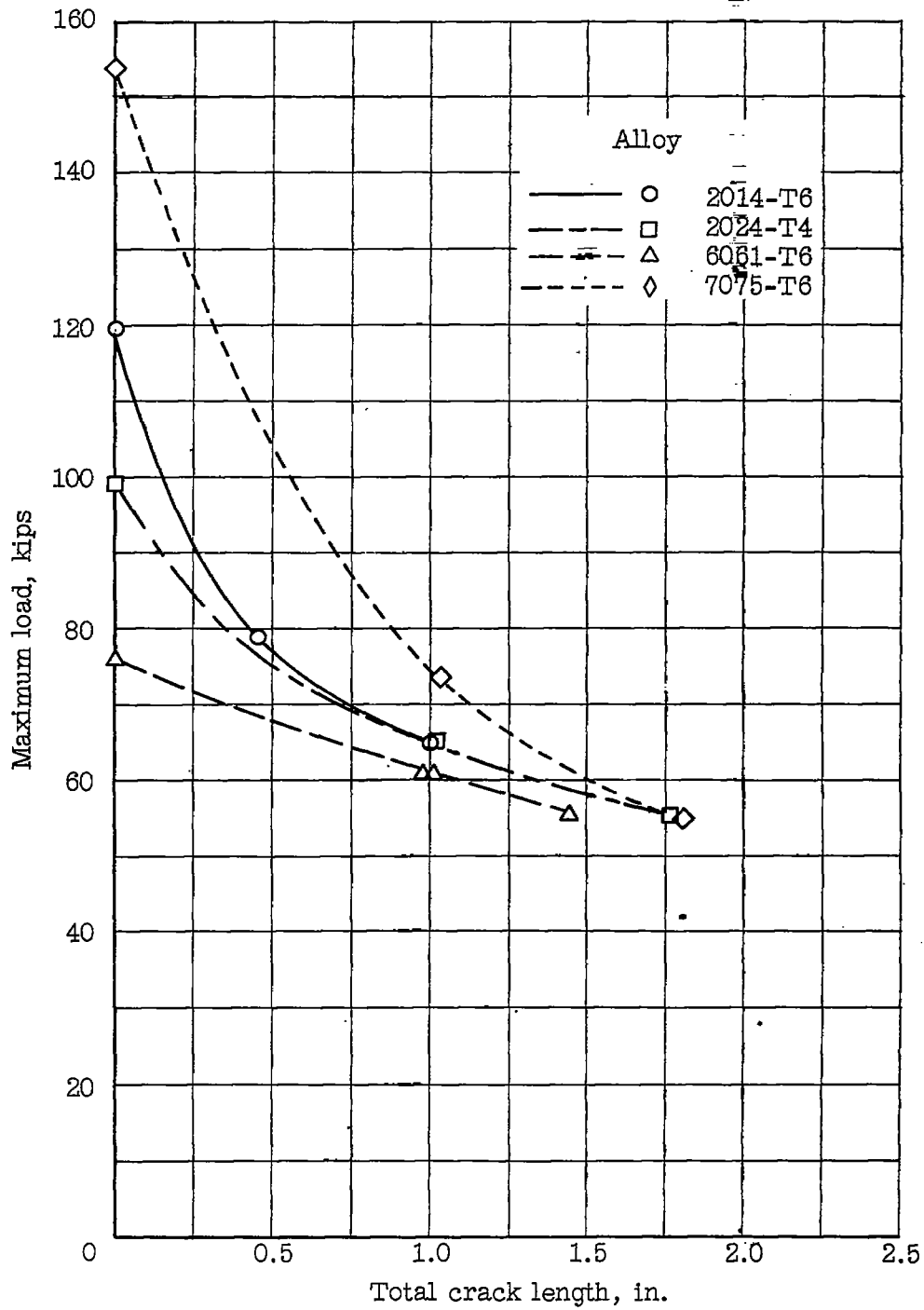


Figure 8.- Effect of length of fatigue crack on ultimate strength of type GX specimens.

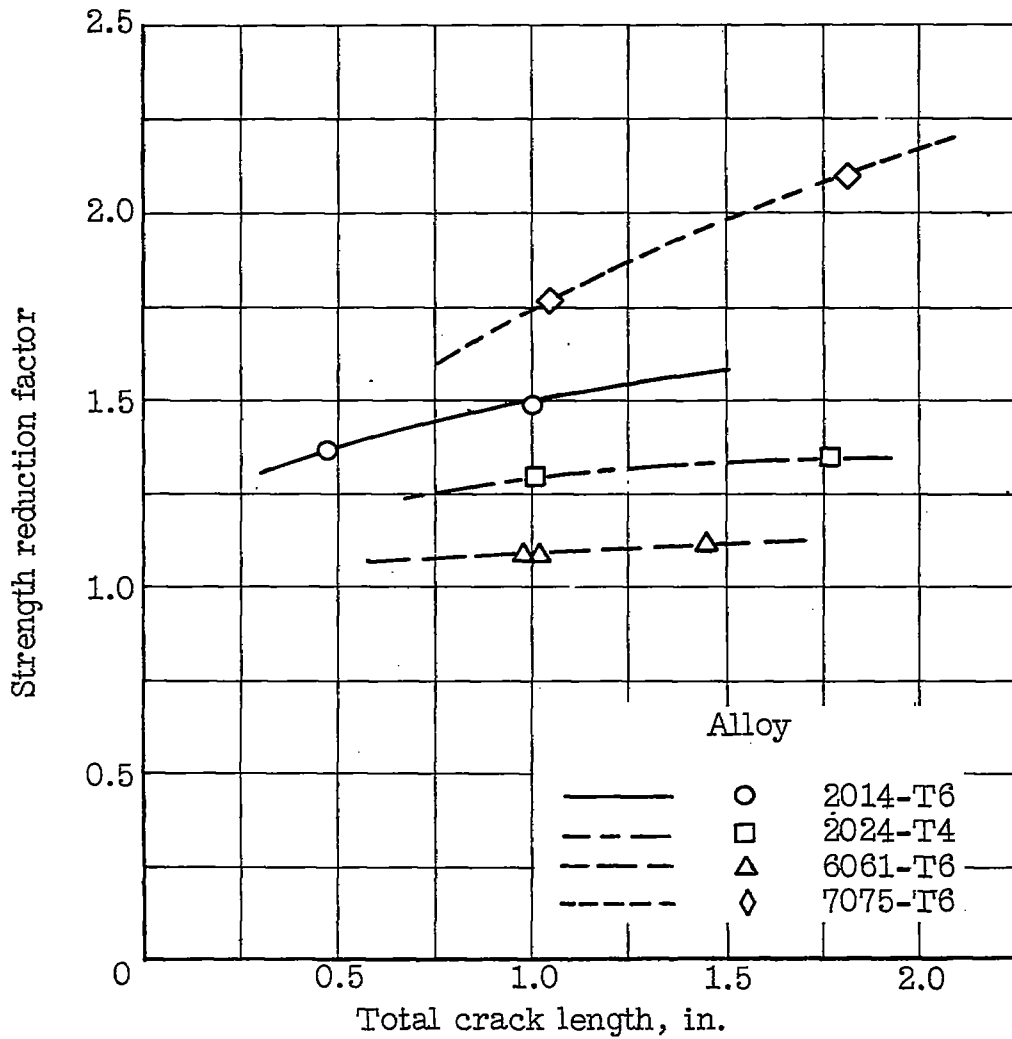


Figure 9.- Variation of strength reduction factors with crack length.

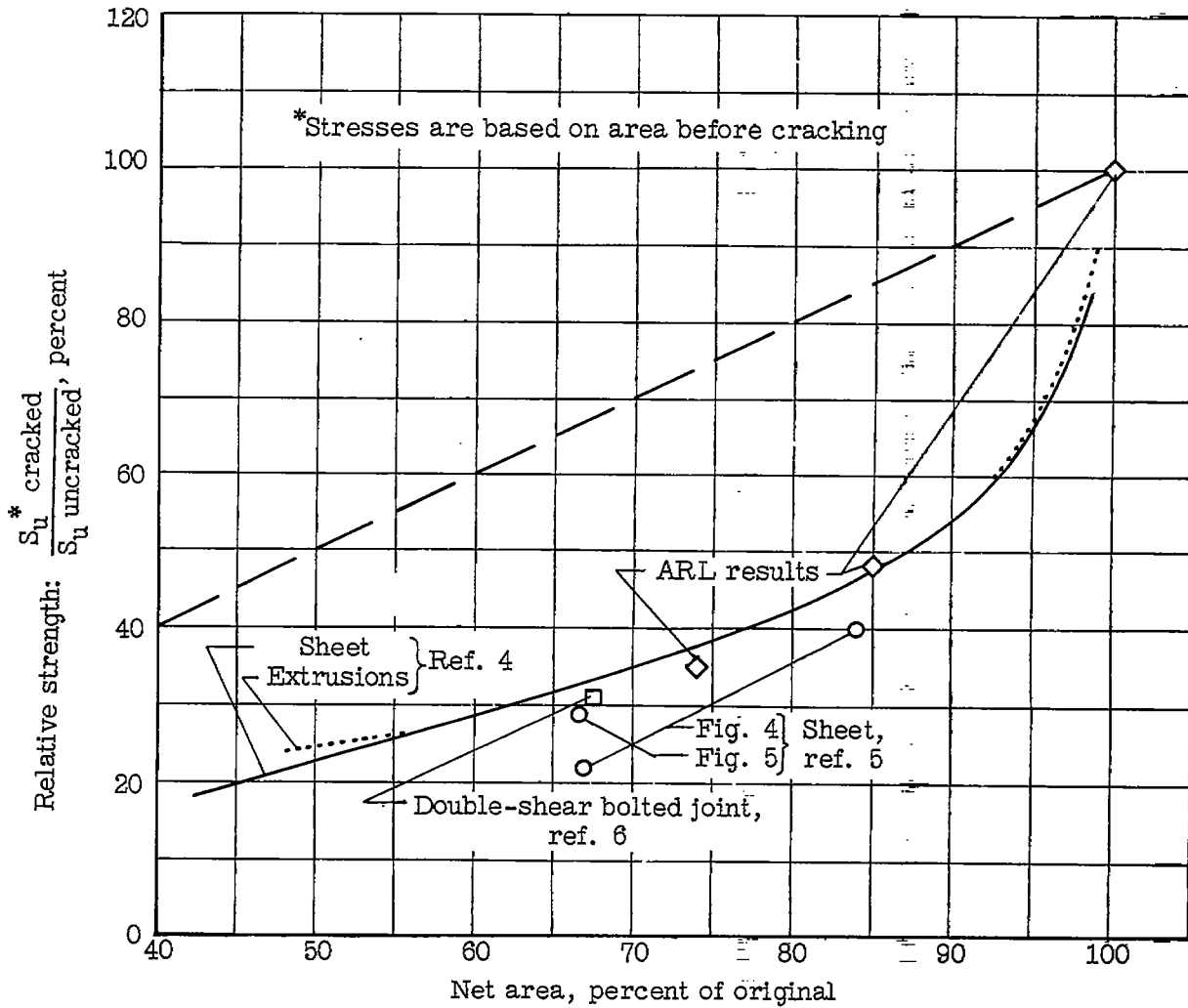


Figure 10.- Comparison of static strength of cracked 7075-T6 aluminum-alloy specimens.

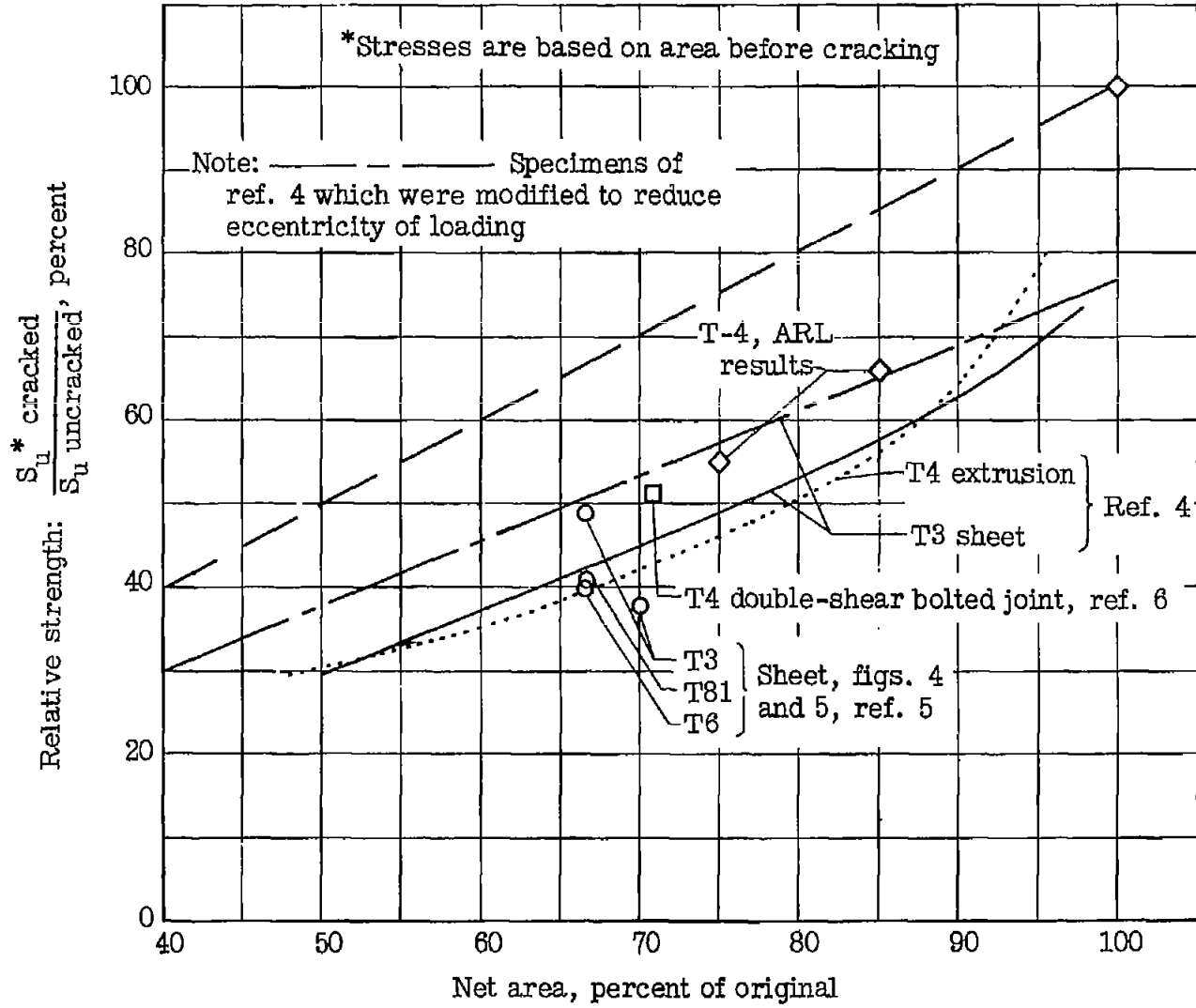


Figure 11.- Comparison of static strengths of cracked 2024 aluminum-alloy specimens.

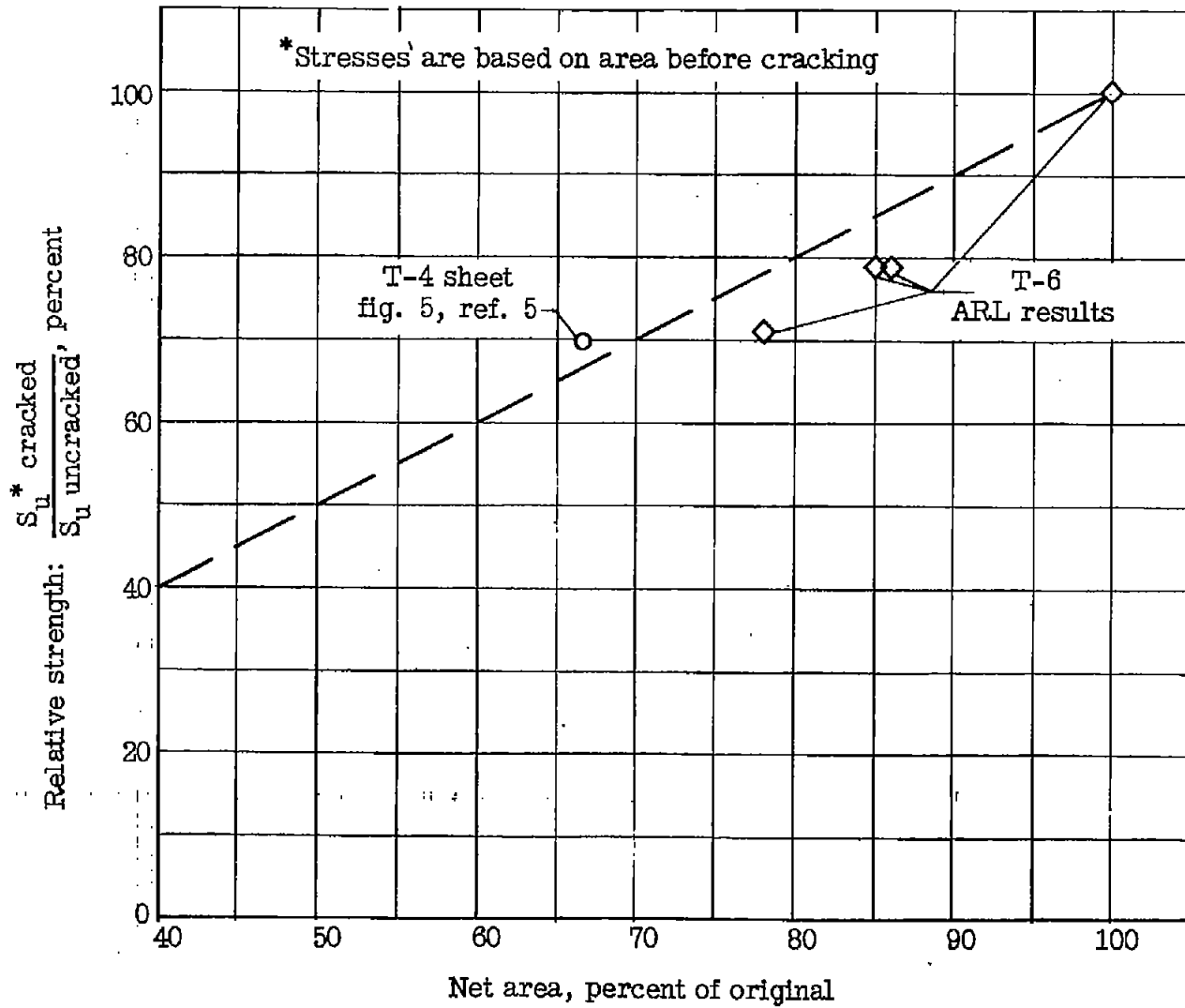
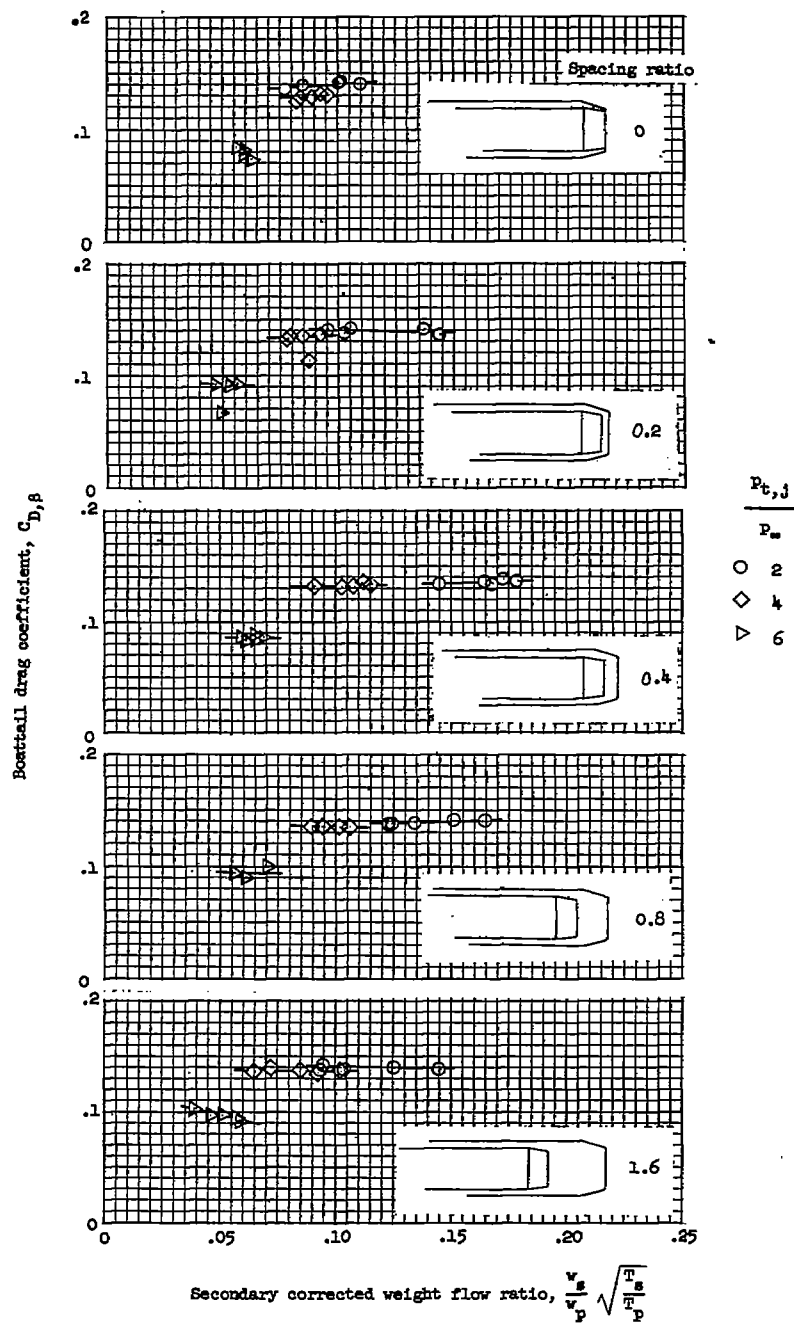


Figure 12.- Comparison of static strengths of cracked 6061 aluminum-alloy specimens.



(c) $M_{\infty} = 1.26$.

Figure 7.- Concluded.

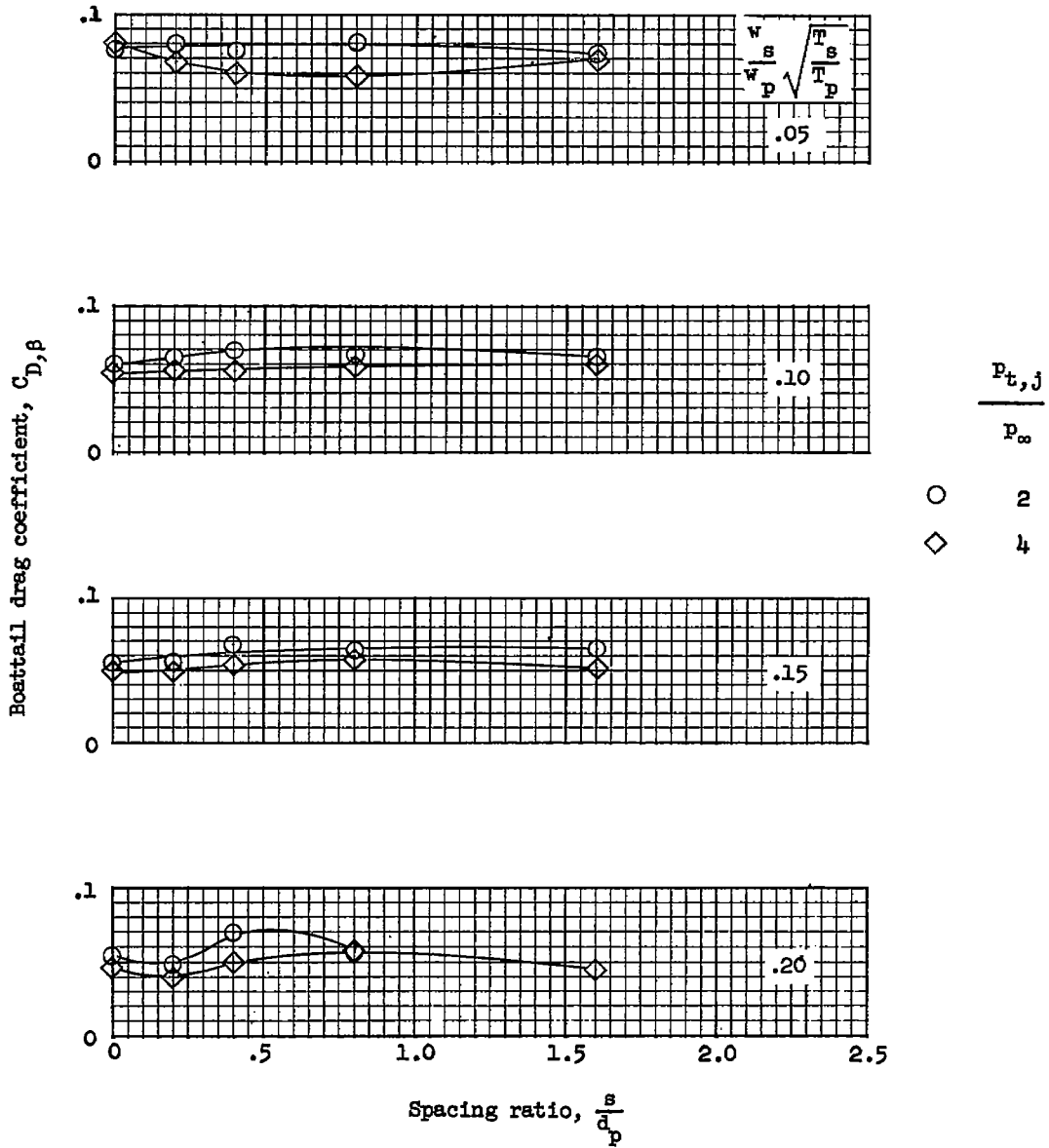
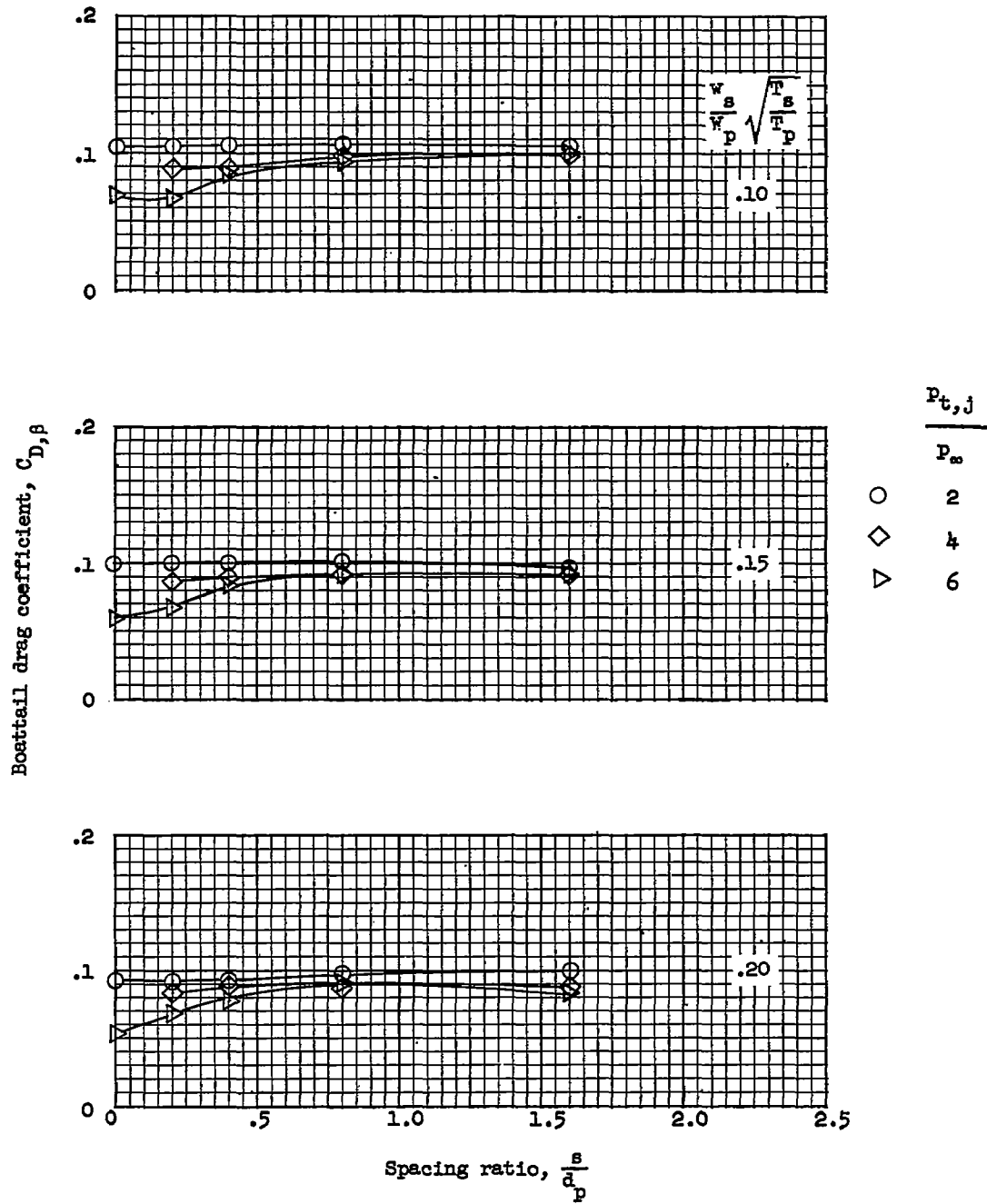
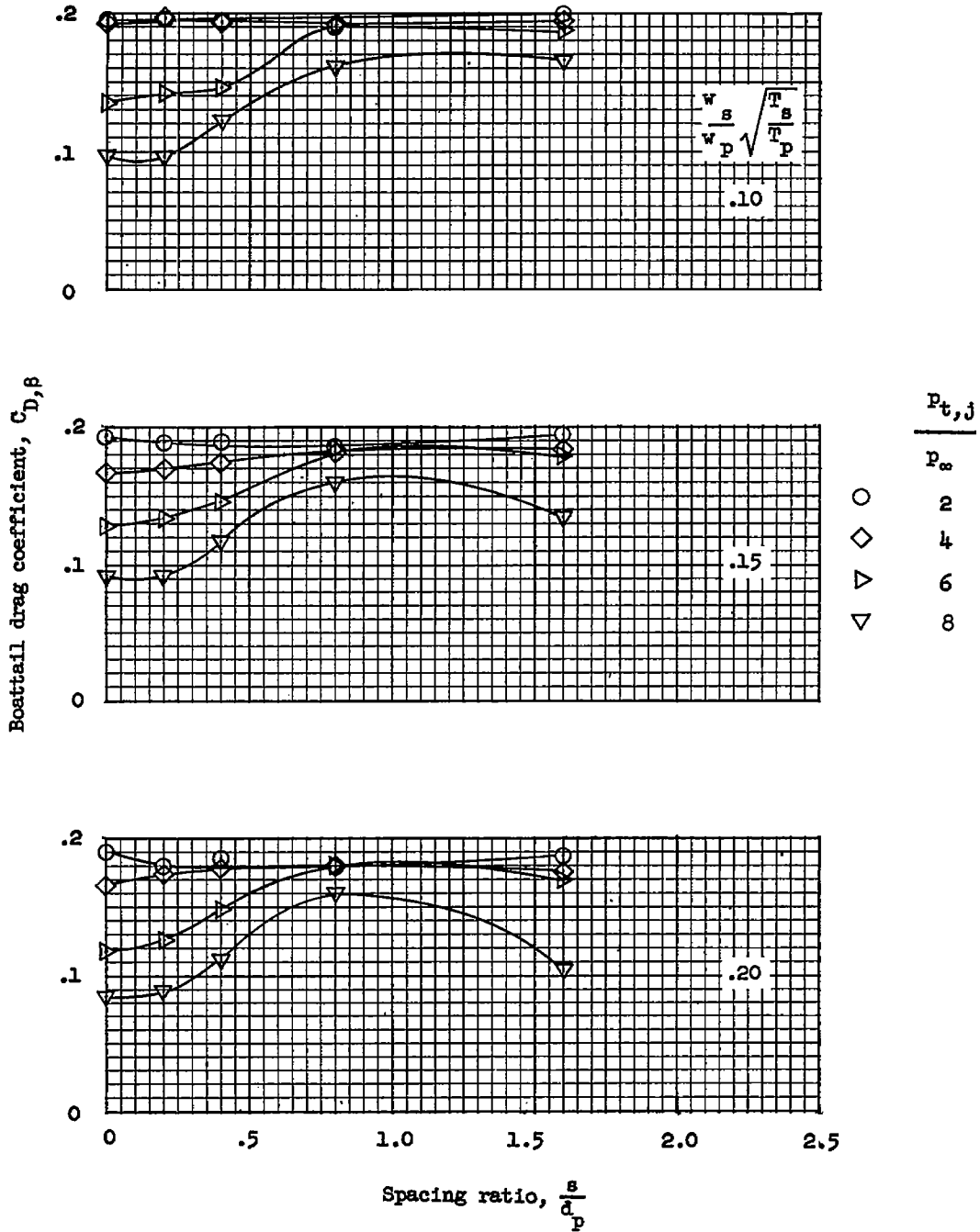
(a) $M_\infty = 0.6$.

Figure 8.- Variation of boattail drag coefficient with spacing ratio at constant values of primary jet total-pressure ratio and secondary mass flow. $\frac{d_s}{d_p} = 1.35$.



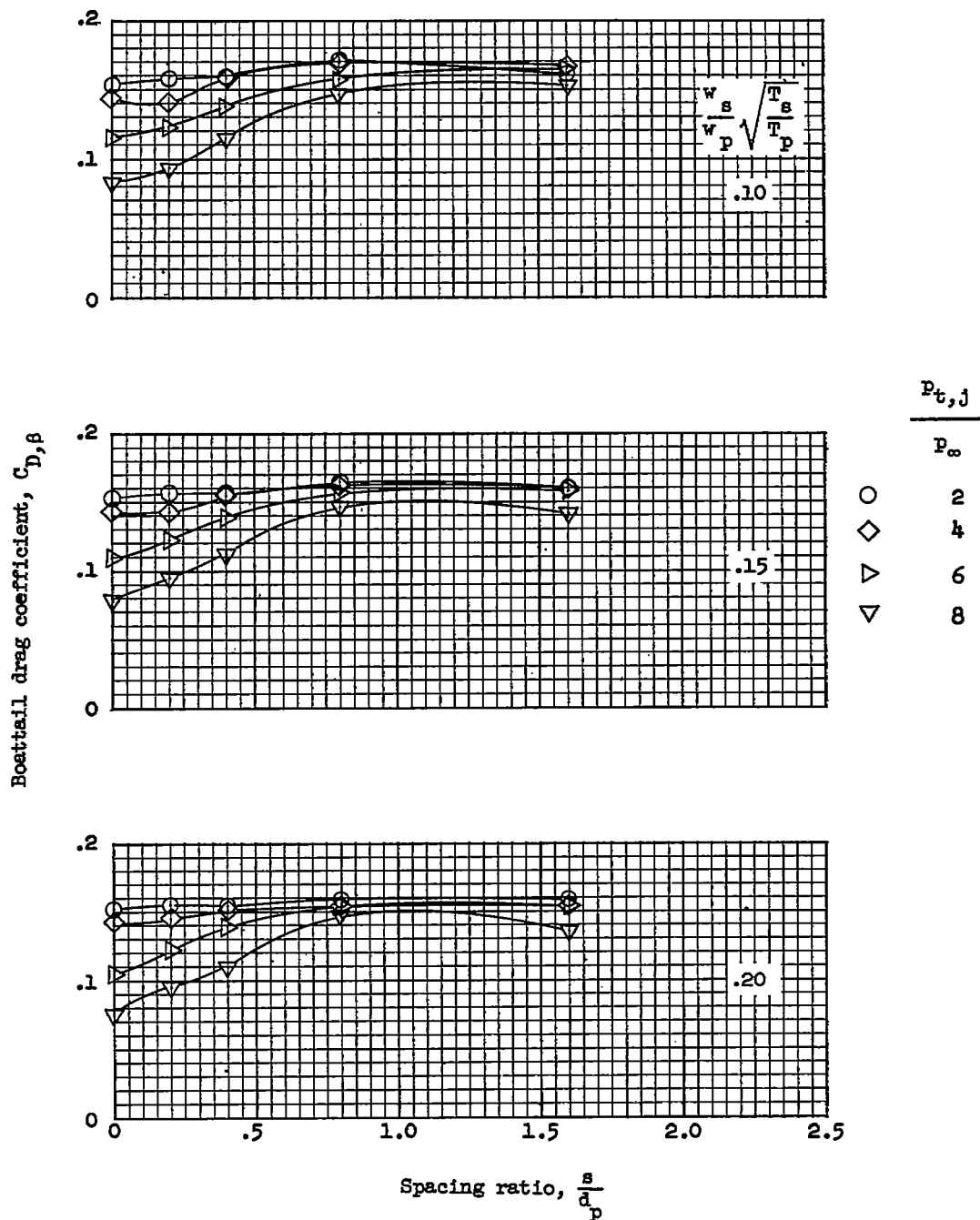
(b) $M_\infty = 0.9$.

Figure 8.- Continued.



(c) $M_{\infty} = 1.10$.

Figure 8.- Continued.



(d) $M_\infty = 1.26$.

Figure 8.- Concluded.

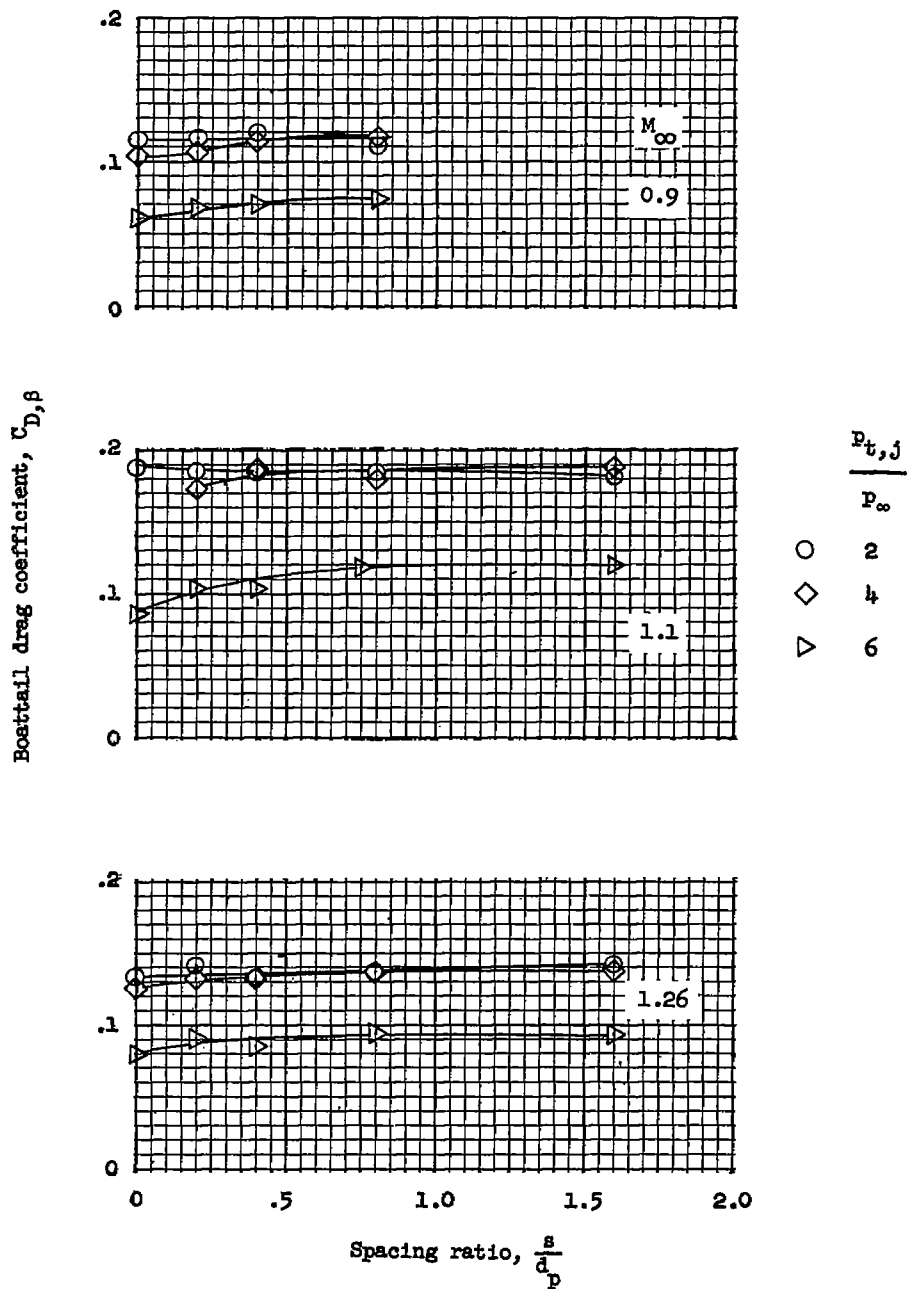
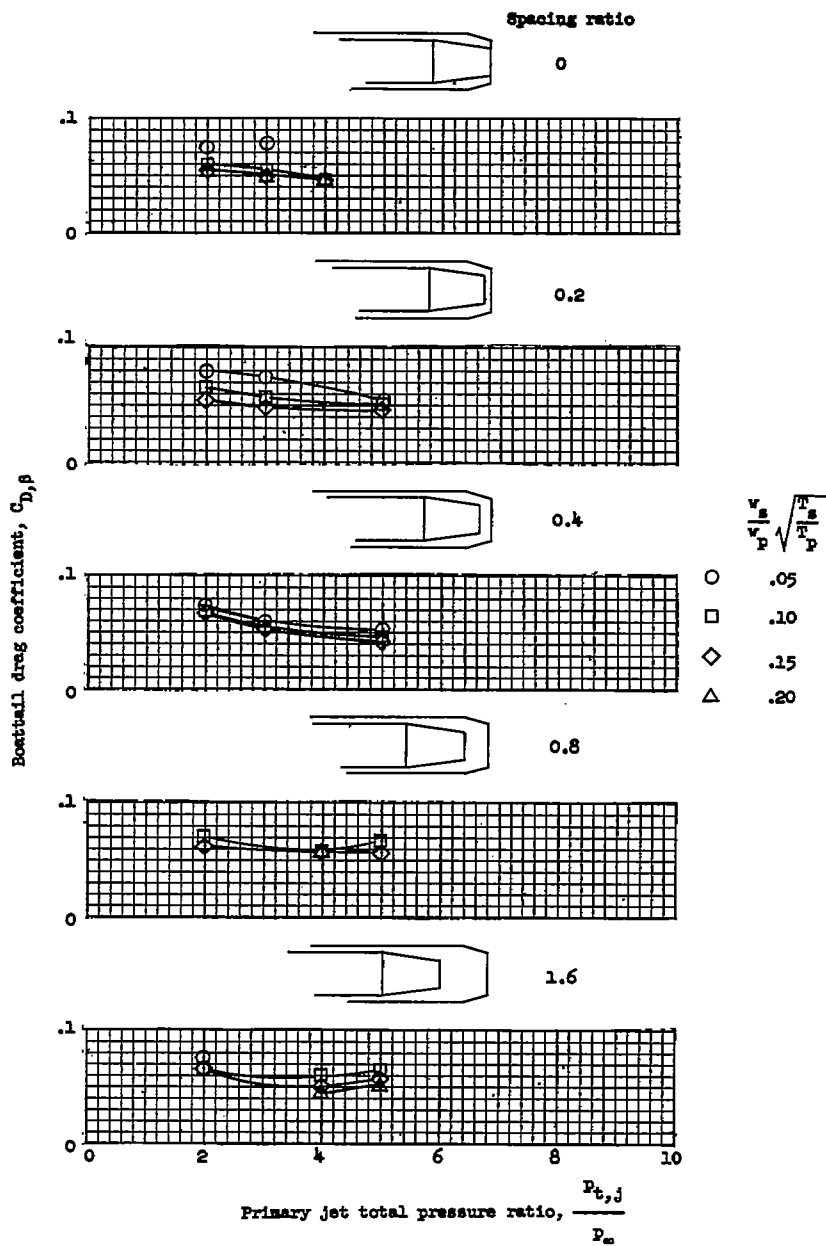


Figure 9.- Variation of boattail drag coefficient with spacing ratio at constant values of primary jet total-pressure ratio.

$$\frac{w_s}{w_p} \sqrt{\frac{T_s}{T_p}} = 0.06; \quad \frac{d_s}{d_p} = 1.10.$$



(a) $M_{\infty} = 0.6$.

Figure 10.- Variation of boattail drag coefficient with primary jet total-pressure ratio at constant values of corrected weight flow and spacing ratio. $\frac{d_s}{d_p} = 1.375$.

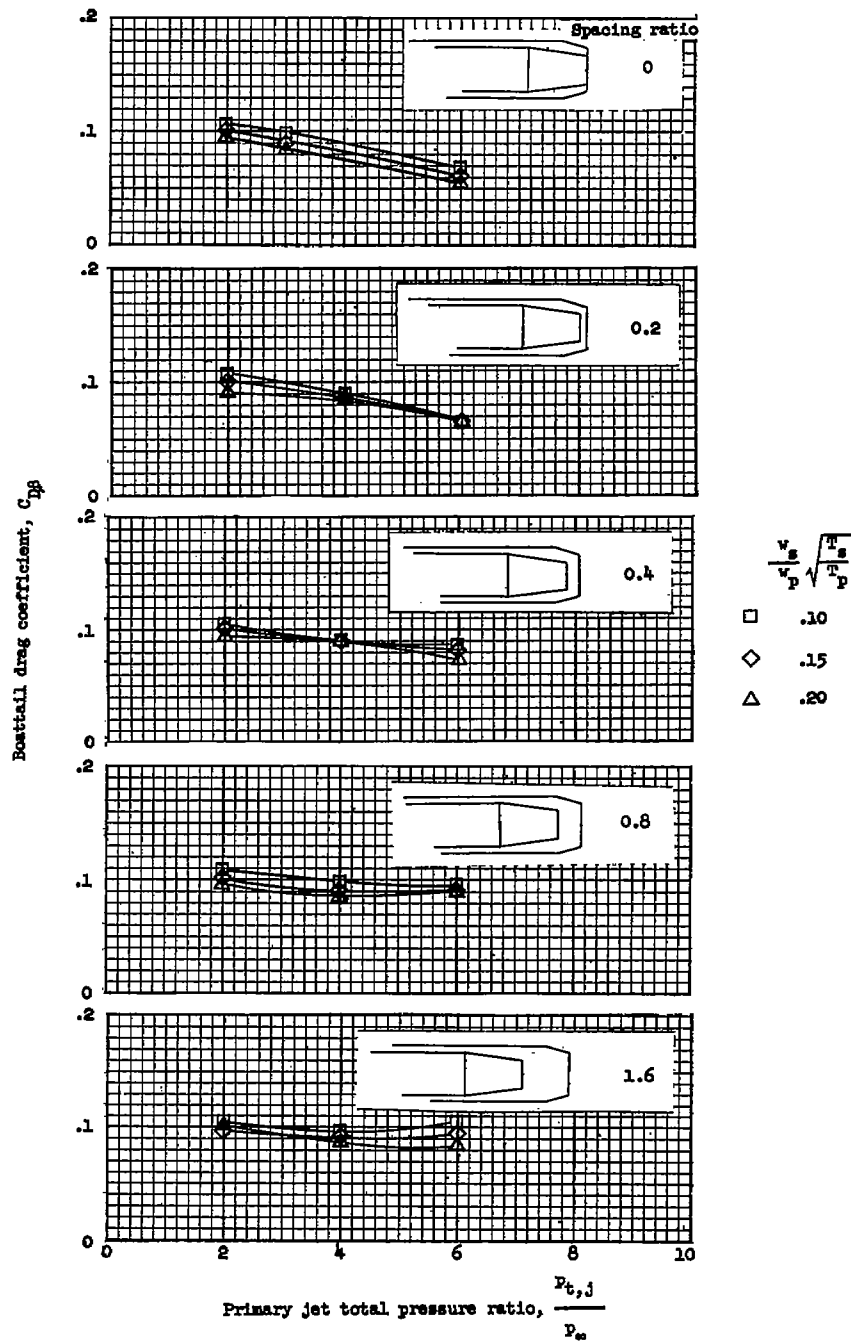
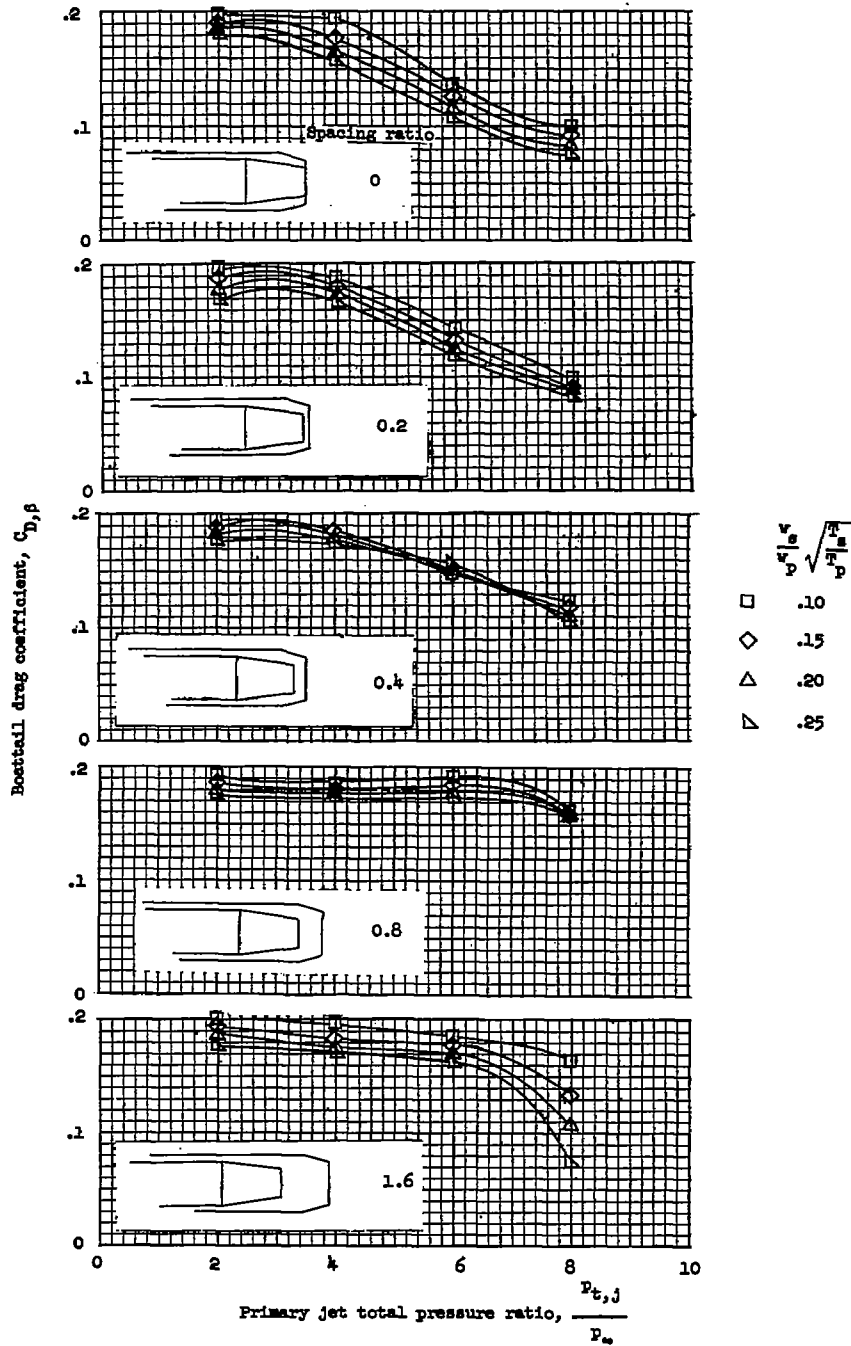
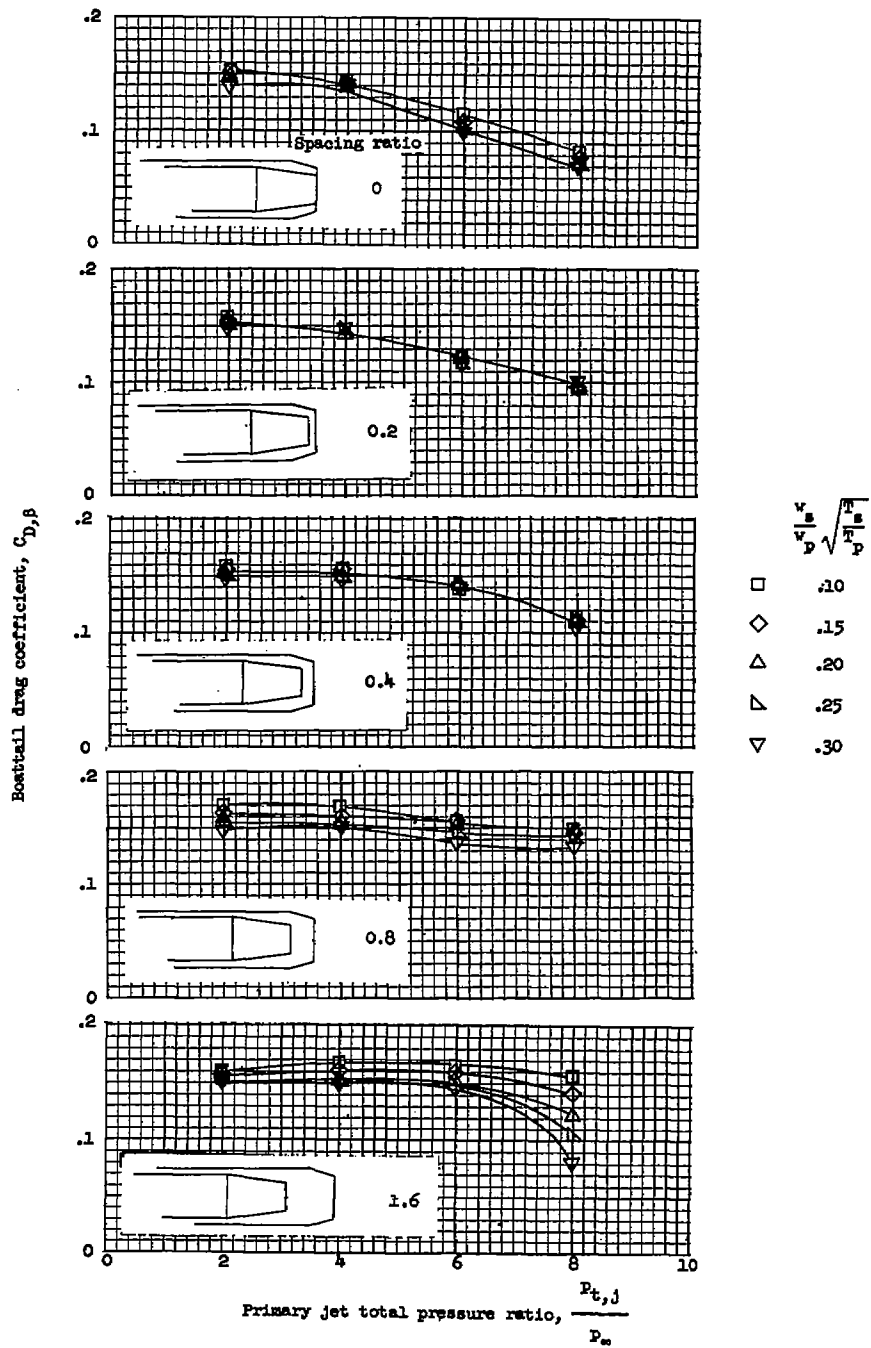
(b) $M_\infty = 0.9$.

Figure 10.- Continued.



(c) $M_\infty = 1.10$.

Figure 10.- Continued.



(d) $M_\infty = 1.26$.

Figure 10.- Concluded.

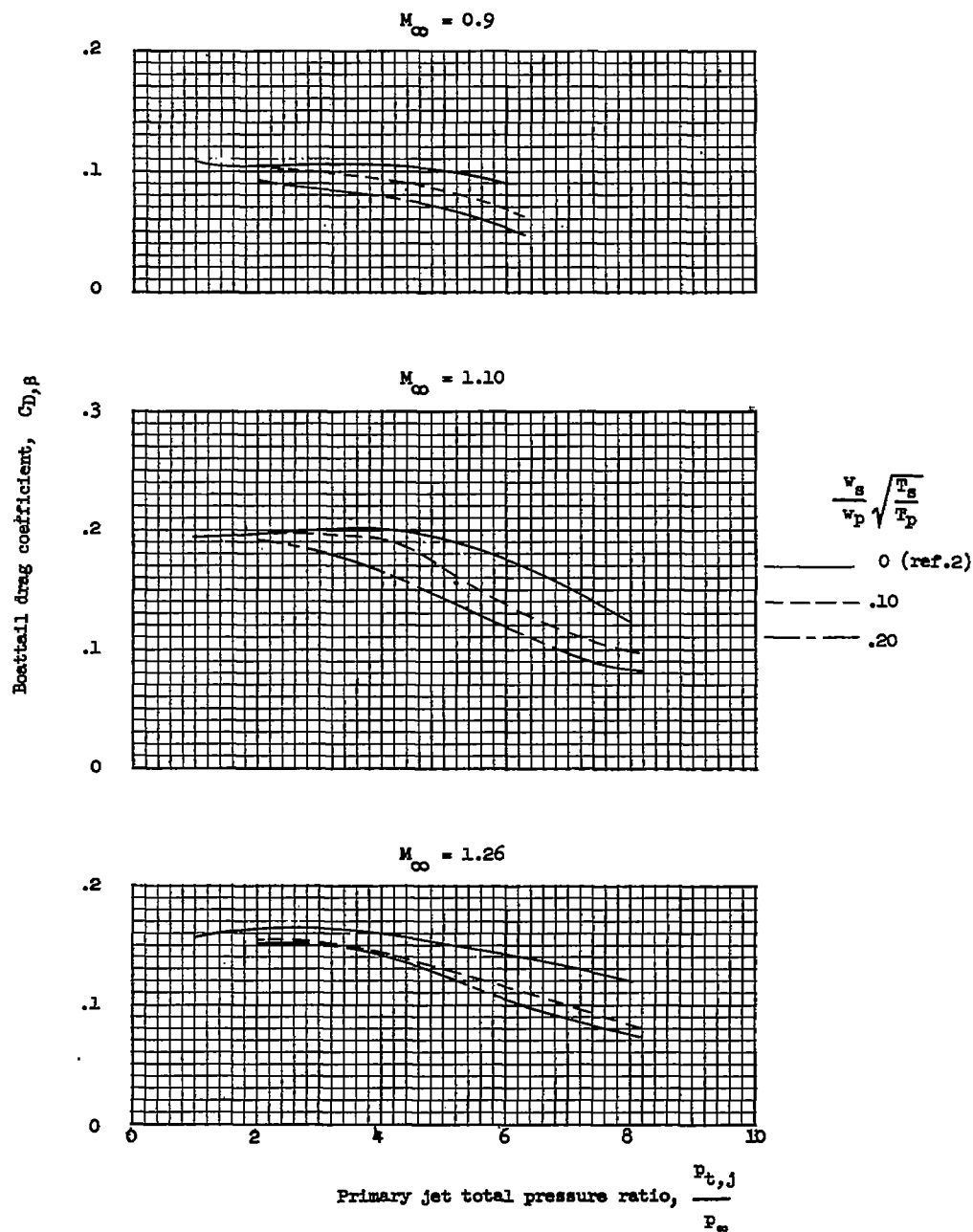
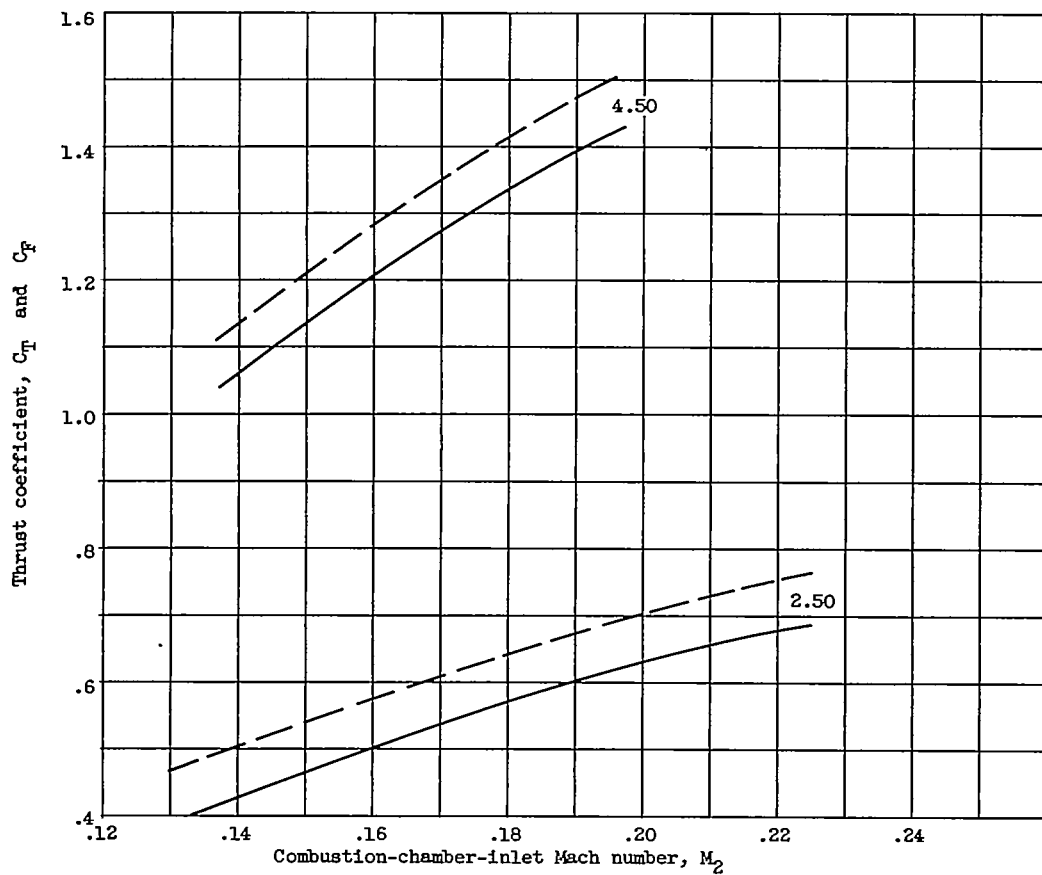
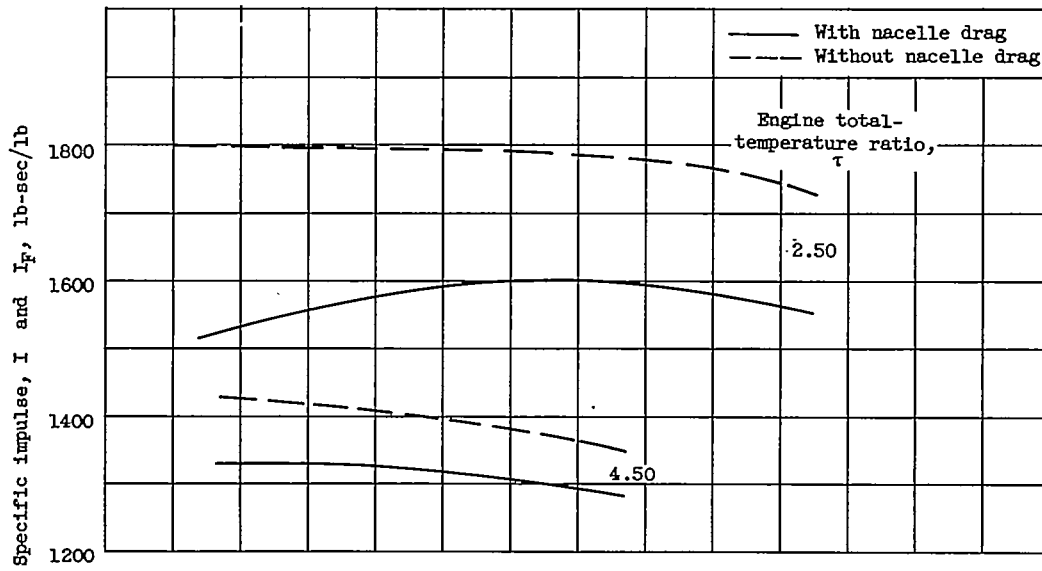


Figure 11.- Comparison with interpolated data from reference 2.

$$\frac{s}{d_p} = 0; \quad \frac{d_b}{d_m} = 0.75; \quad \frac{d_p}{d_b} = 0.67; \quad \beta = 16^\circ.$$

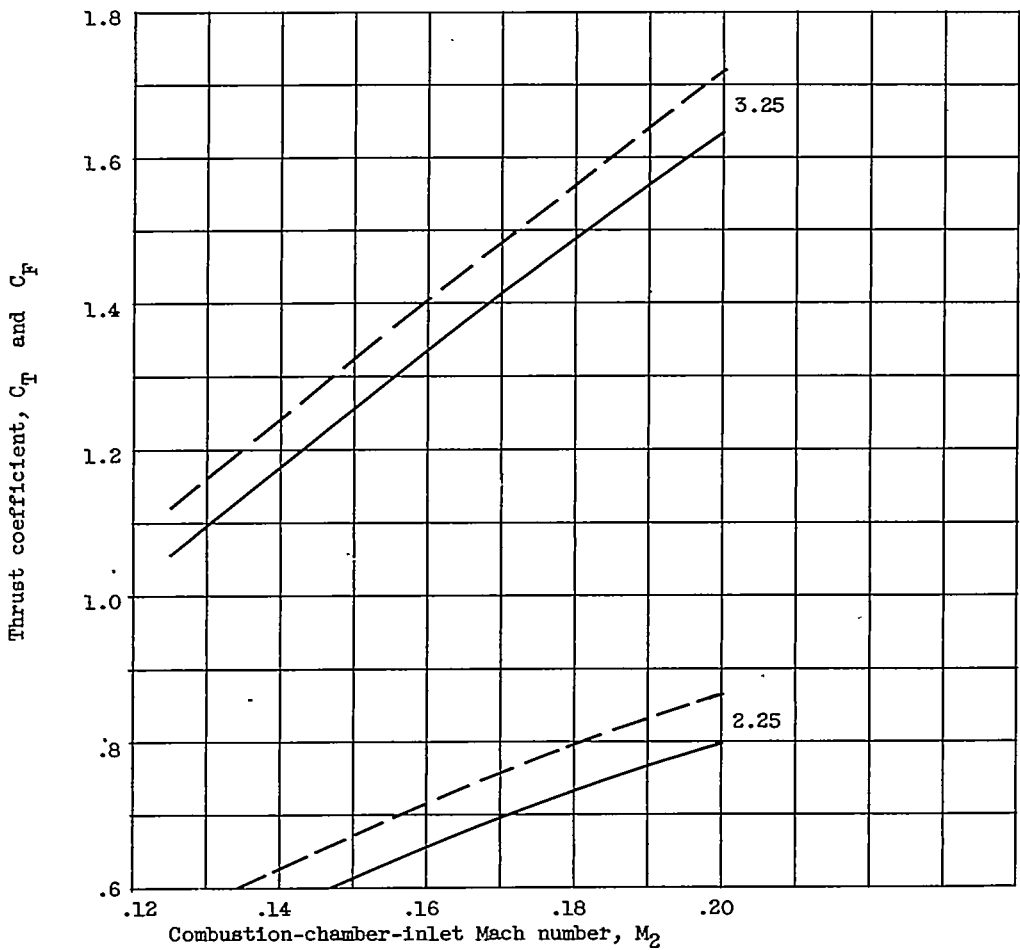
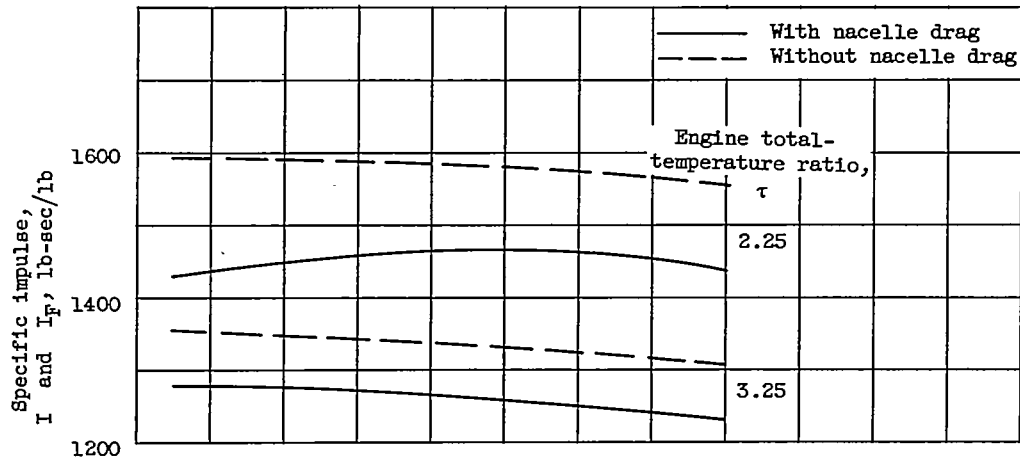
CR-5 back 3302



(a) Flight Mach number, 2.5.

Figure 6. - Effect of combustion-chamber-inlet Mach number on ram-jet engine performance.

~~CONFIDENTIAL~~



(b) Flight Mach number, 3.5.

Figure 6. - Concluded. Effect of combustion-chamber-inlet Mach number on ram-jet engine performance.

~~CONFIDENTIAL~~

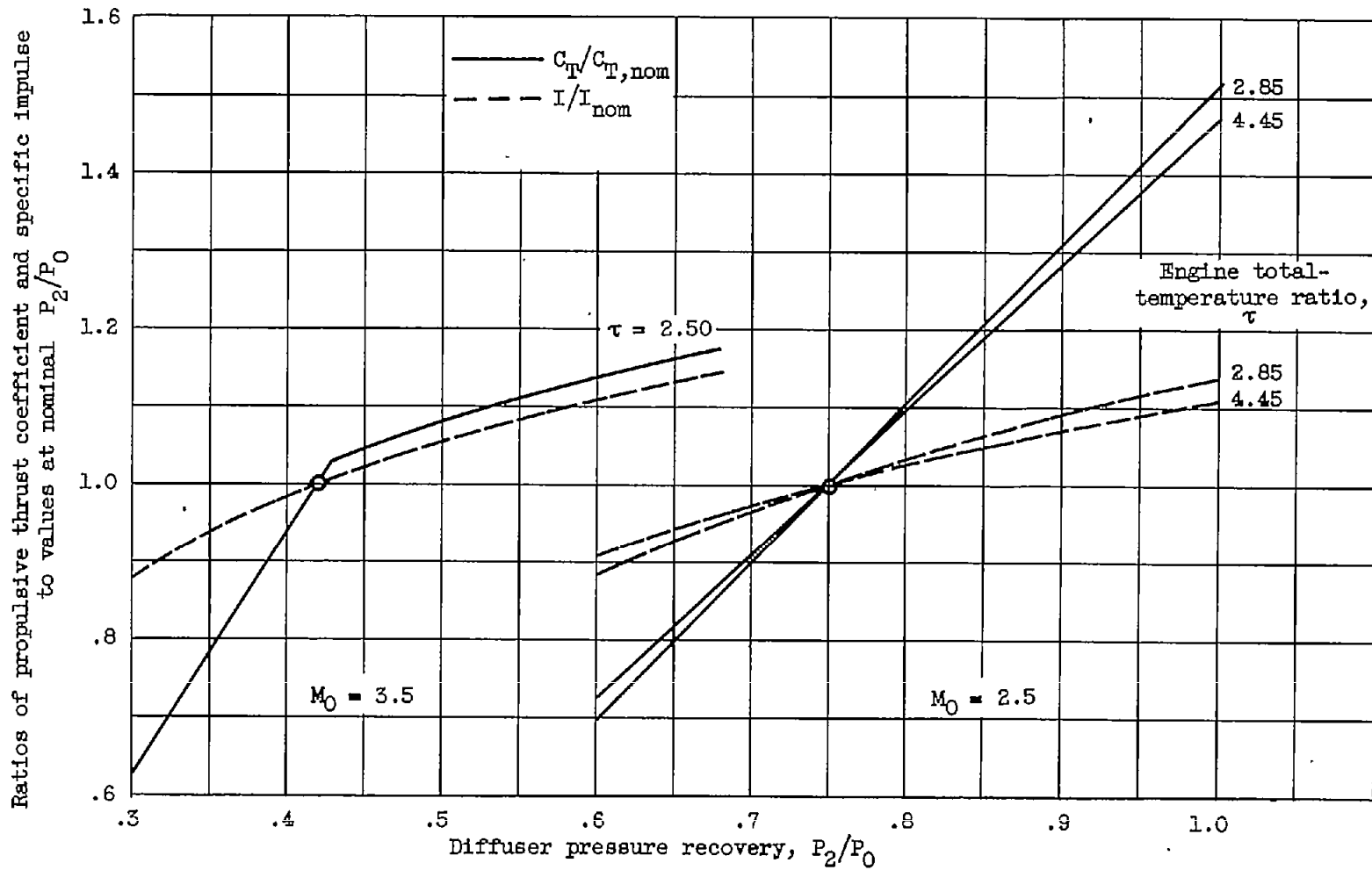


Figure 7. - Effect of diffuser pressure recovery on ram-jet engine performance. Combustion-chamber-inlet Mach number, 0.200.

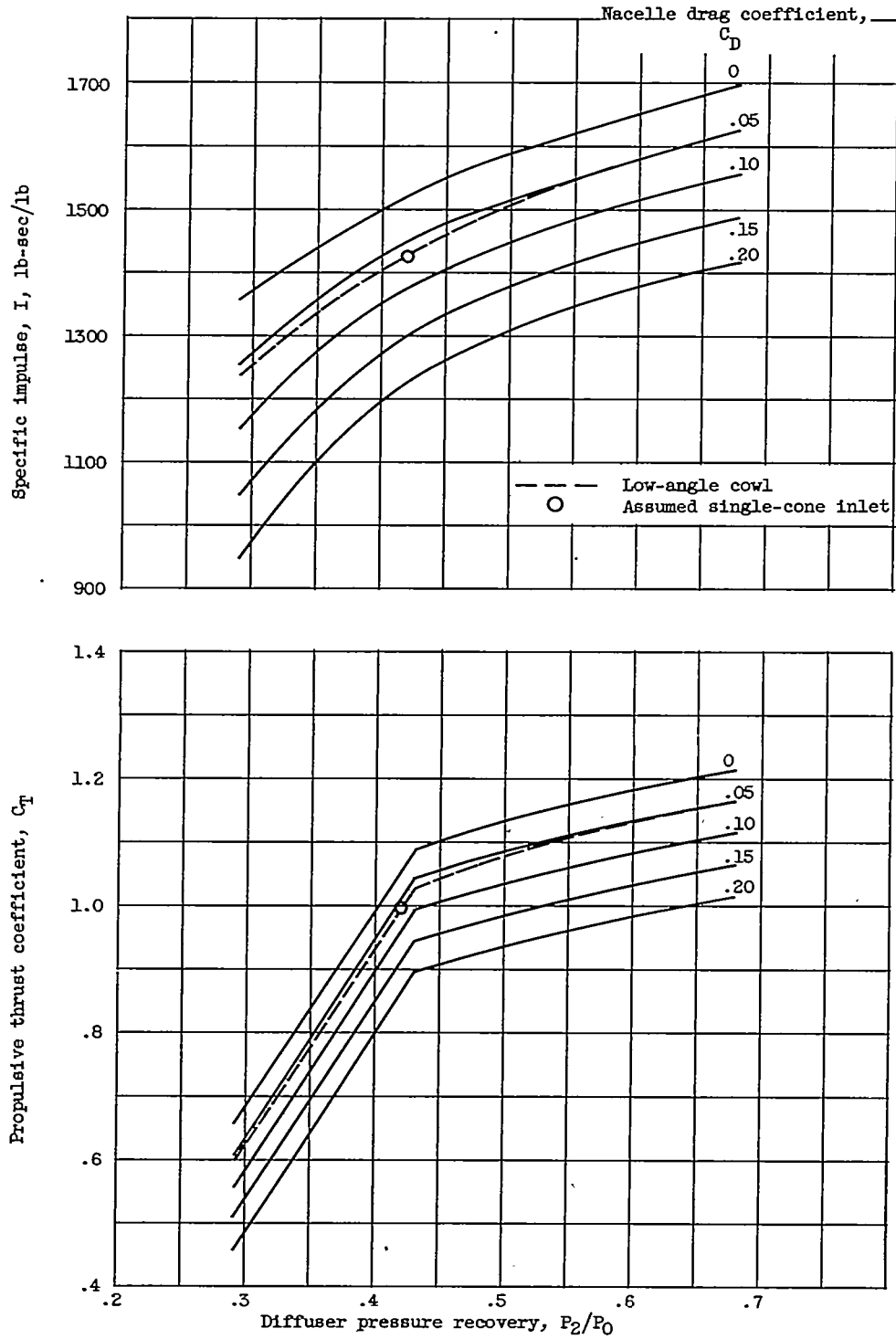


Figure 8. - Effect of diffuser pressure recovery and engine drag coefficient on ram-jet engine performance. Flight Mach number, 3.5; combustion-chamber-inlet Mach number, 0.200; engine total-temperature ratio, 2.50.

~~CONFIDENTIAL~~

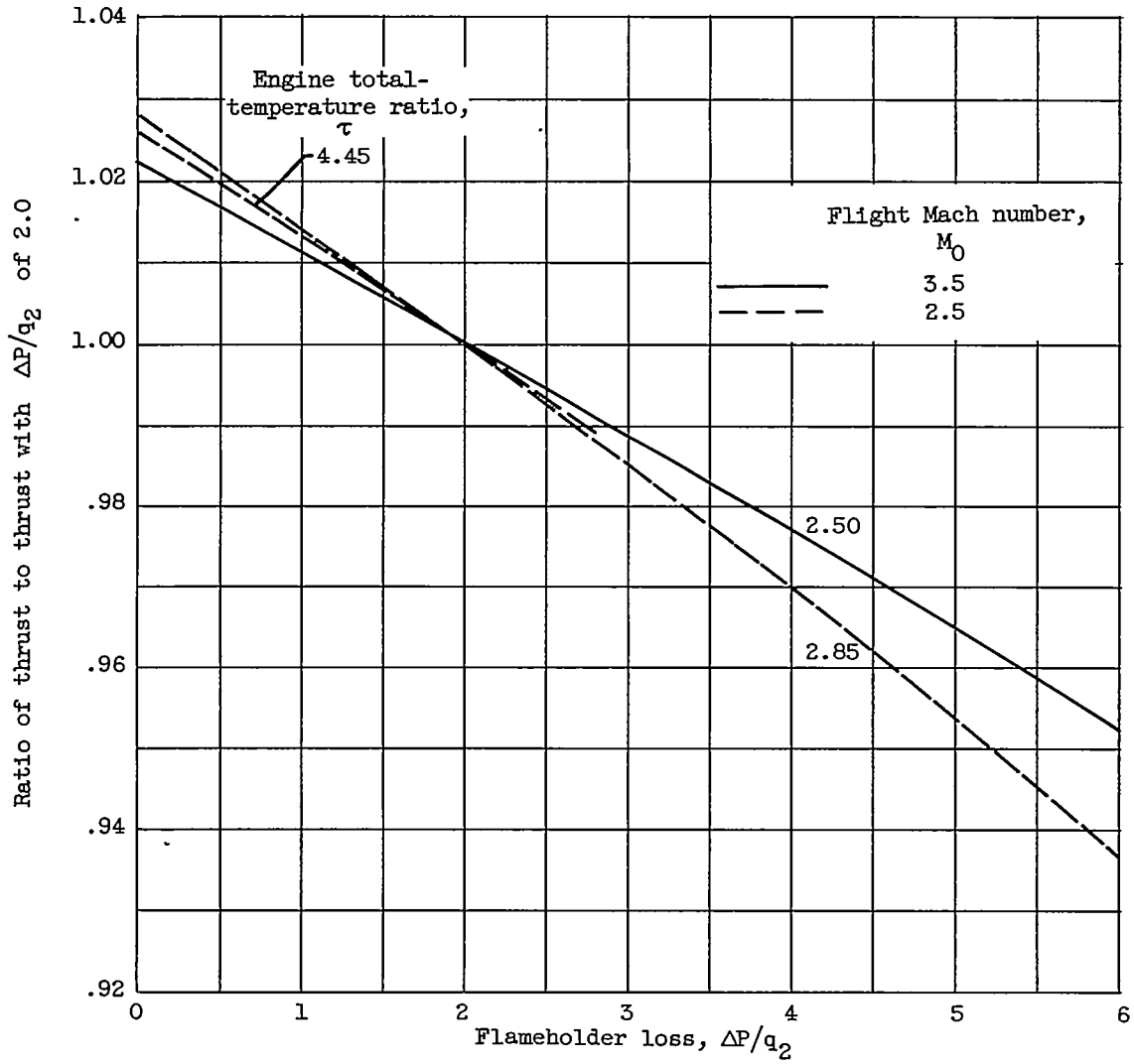


Figure 9. - Effect of flameholder pressure loss on ram-jet engine performance. Combustion-chamber-inlet Mach number, 0.200; combustion efficiency, 0.90. (Specific impulse is affected in same proportion as thrust.)

~~CONFIDENTIAL~~

~~CONFIDENTIAL~~

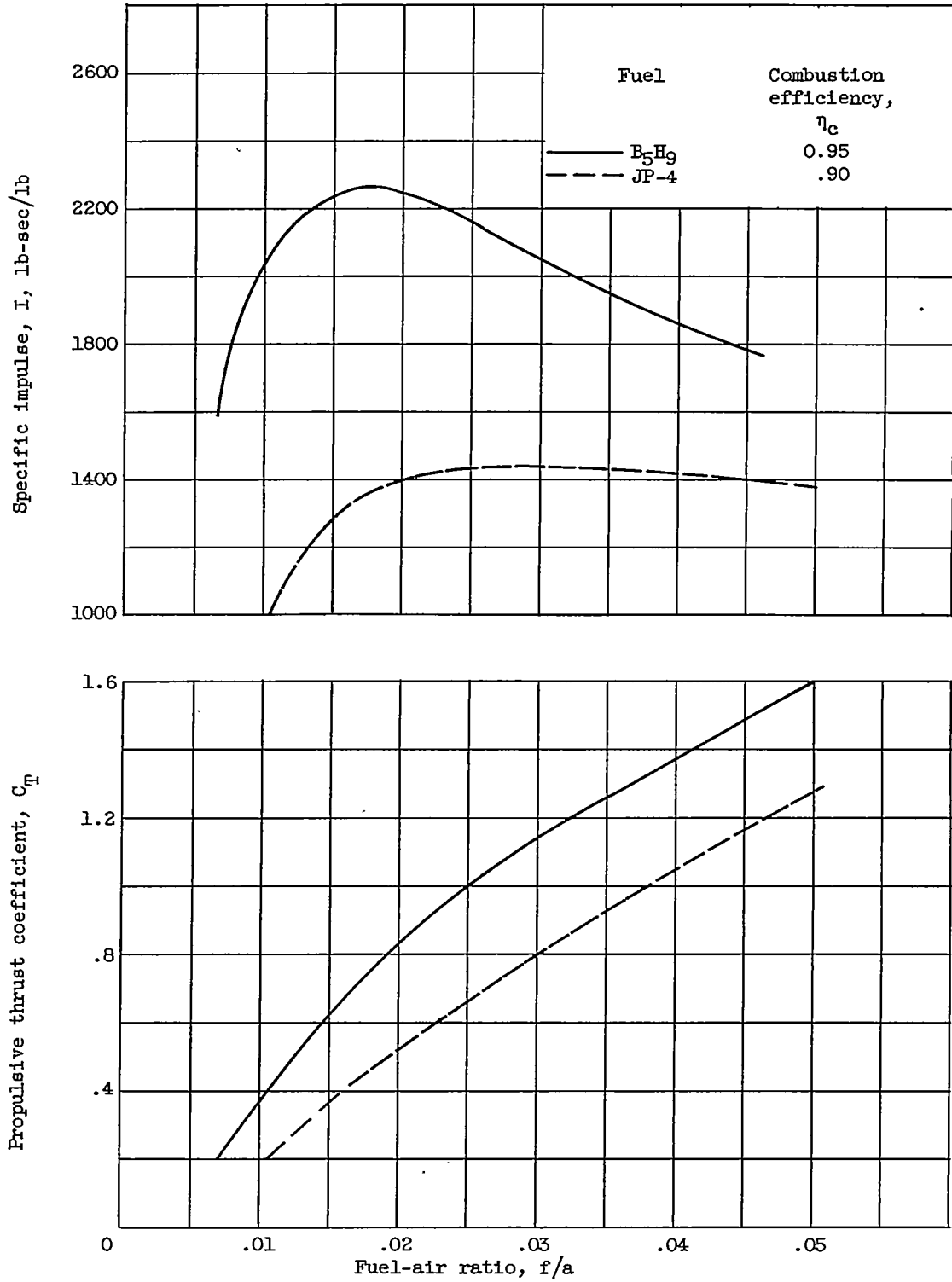


Figure 10. - Comparison between performance of engines using pentaborane and JP-4 fuel. Flight Mach number, 3.5; combustion-chamber-inlet Mach number, 0.200.

~~CONFIDENTIAL~~

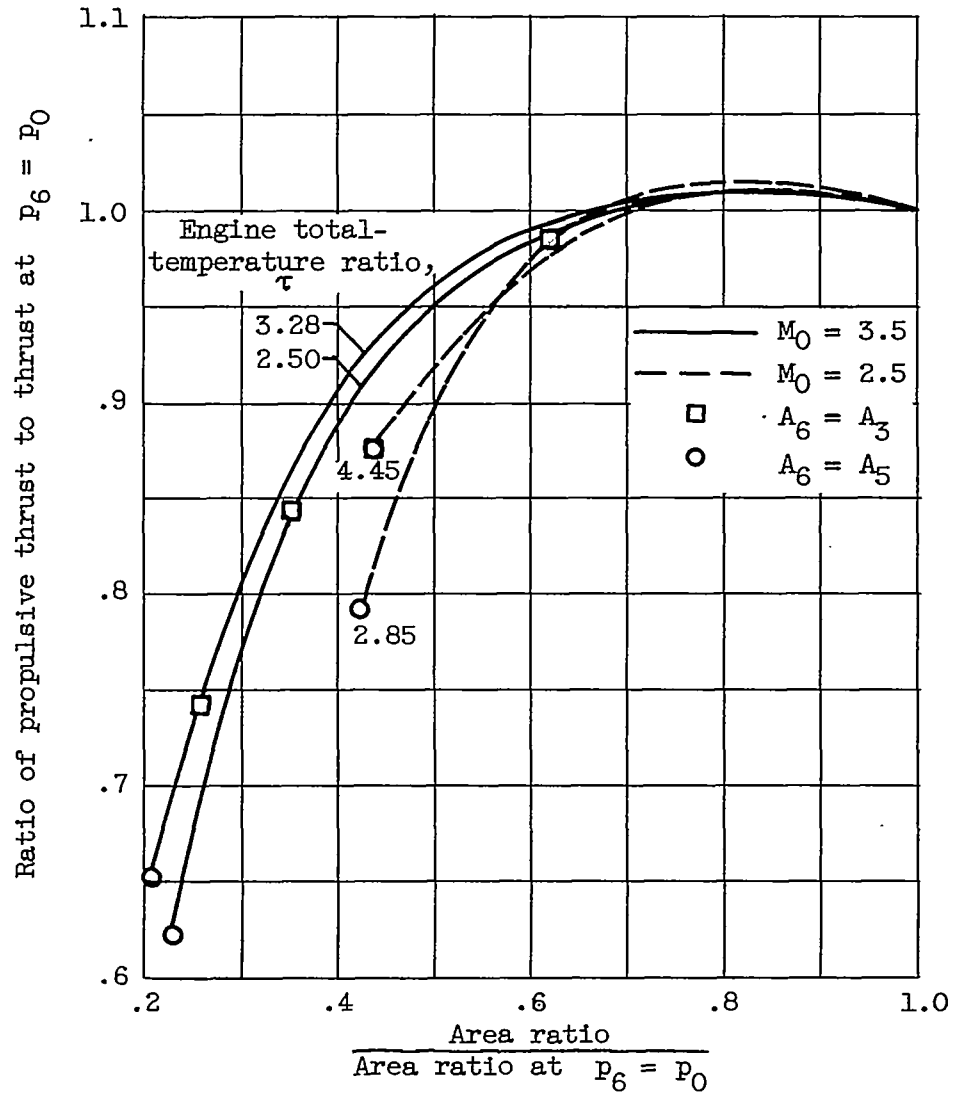


Figure 11. - Effect of nozzle area ratio on ram-jet engine performance. Combustion-chamber-inlet Mach number, 0.200. (Specific impulse is affected in same proportion as thrust.)

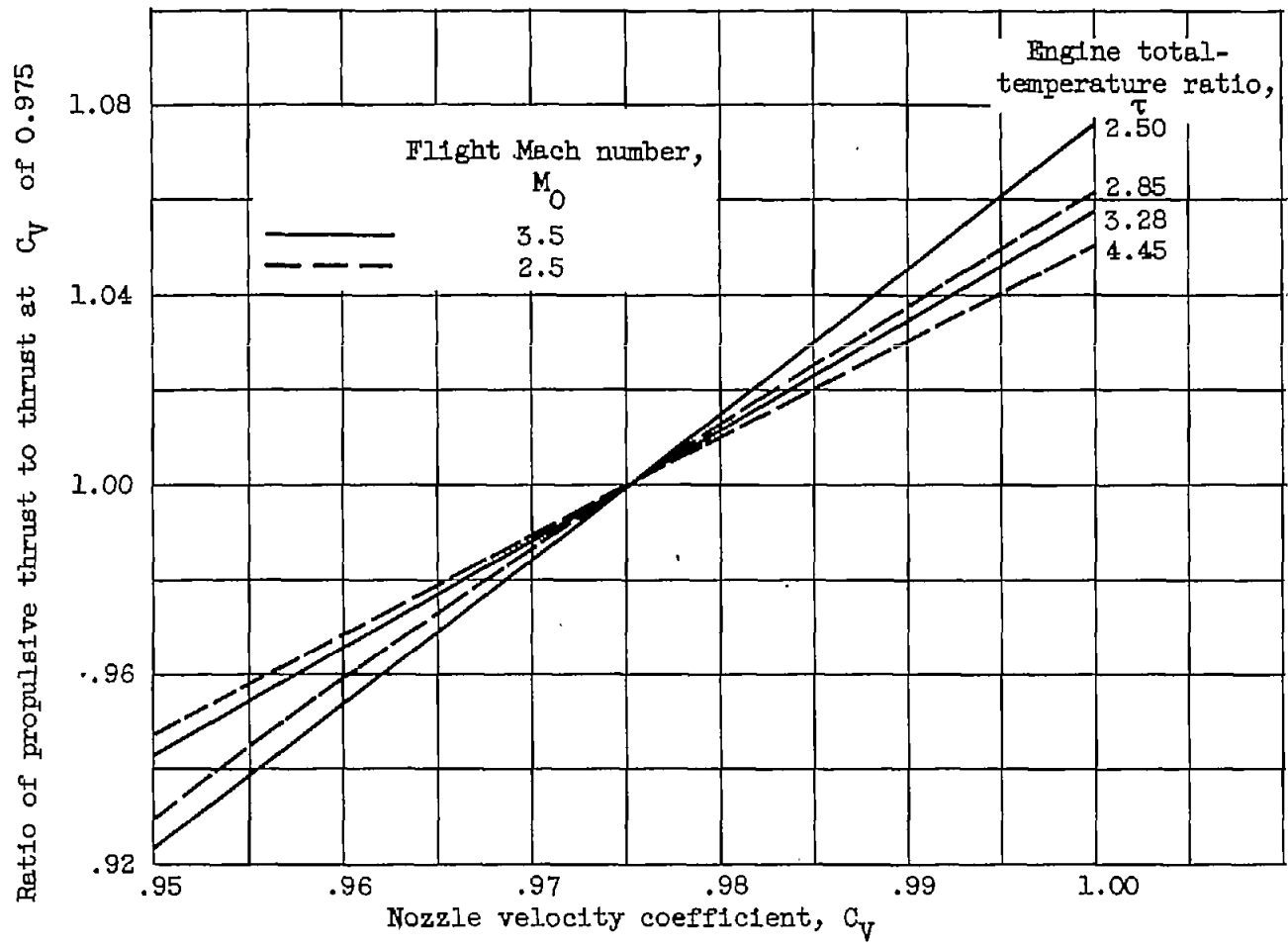


Figure 12. - Effect of nozzle velocity coefficient on ram-jet engine performance. Combustion-chamber-inlet Mach number, 0.200. (Specific impulse is affected in same proportion as thrust.)



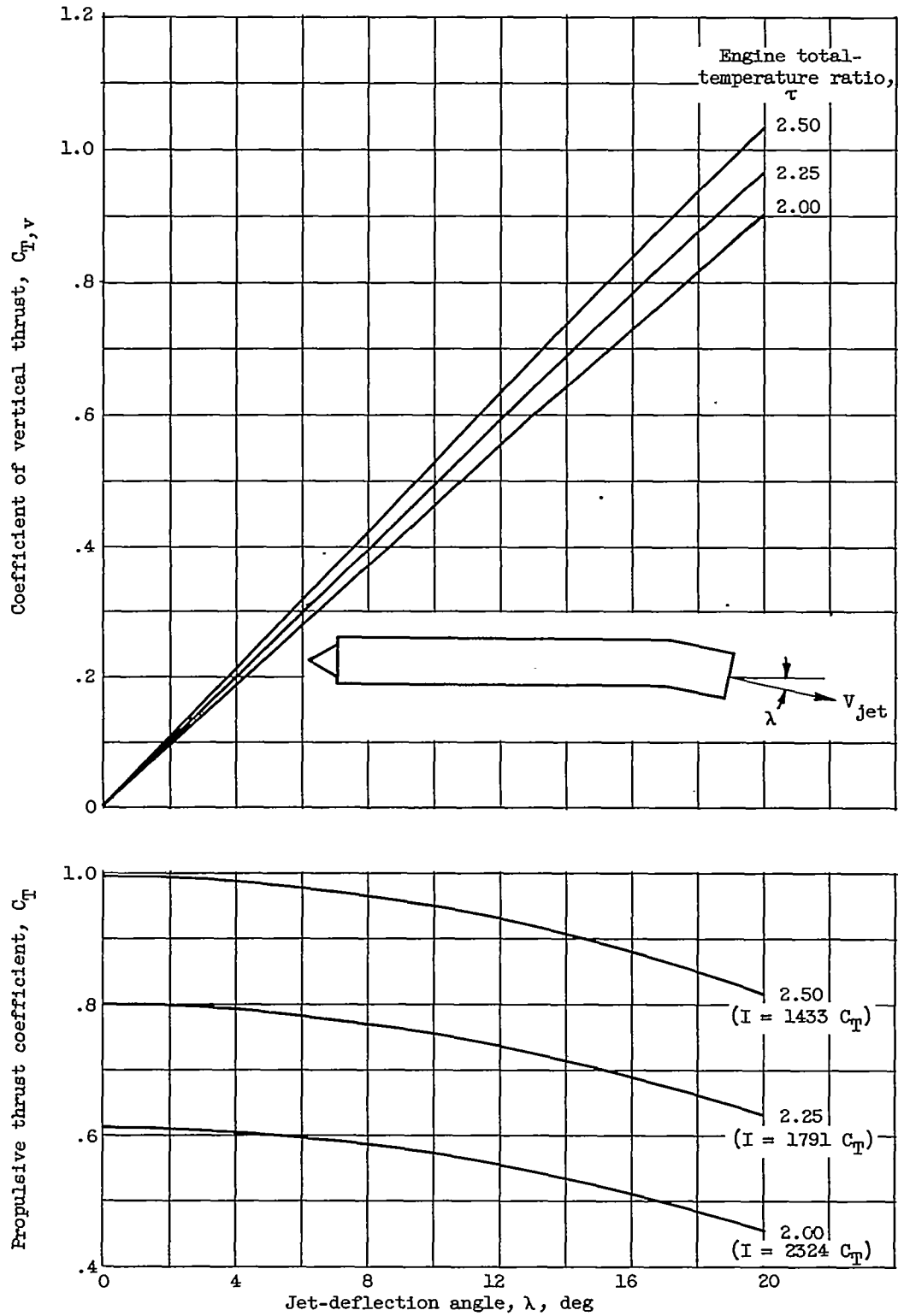


Figure 13. - Effect of jet-deflection angle on ram-jet engine performance. Flight Mach number, 3.5; combustion-chamber-inlet Mach number, 0.200.

~~CONFIDENTIAL~~

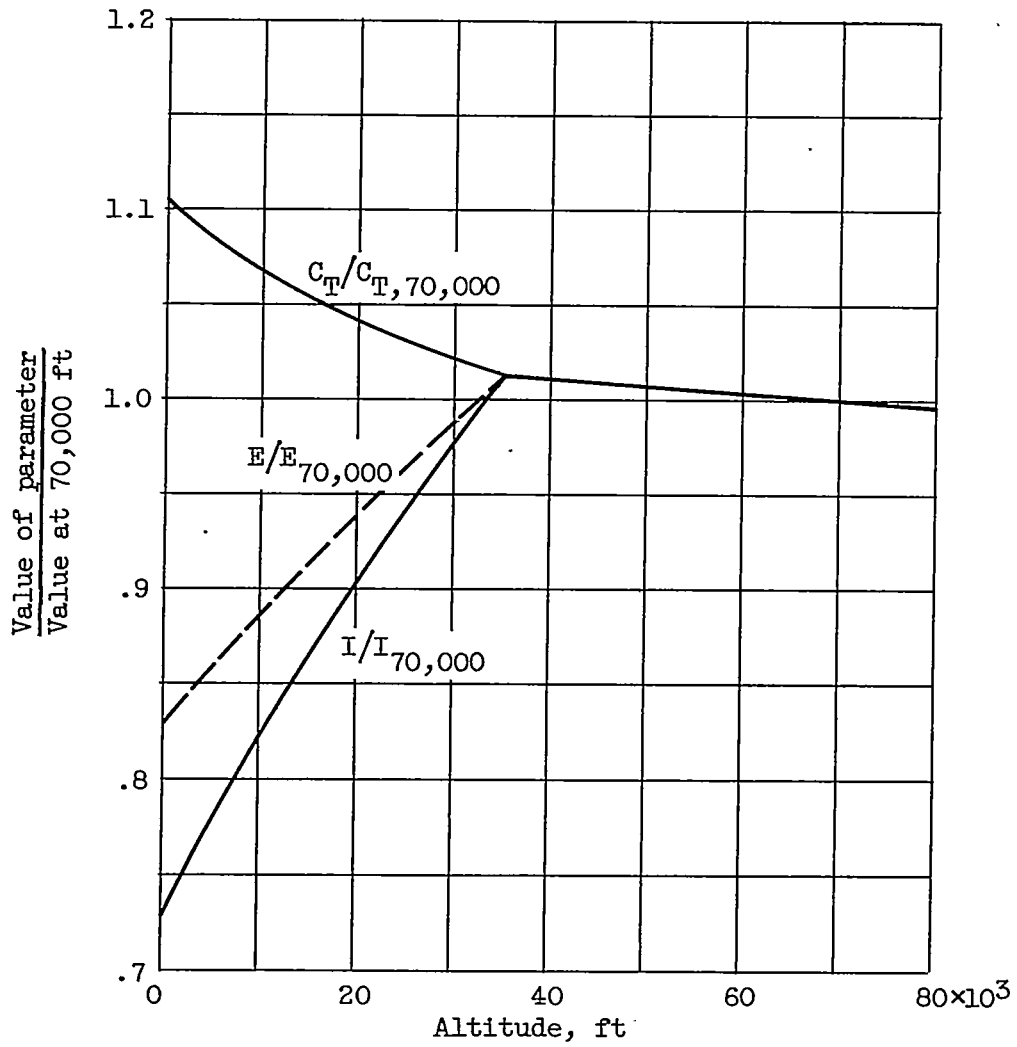


Figure 14. - Effect of altitude on ram-jet engine performance. Flight Mach number, 3.5; combustion-chamber-inlet Mach number, 0.200; engine total-temperature ratio, 2.50.

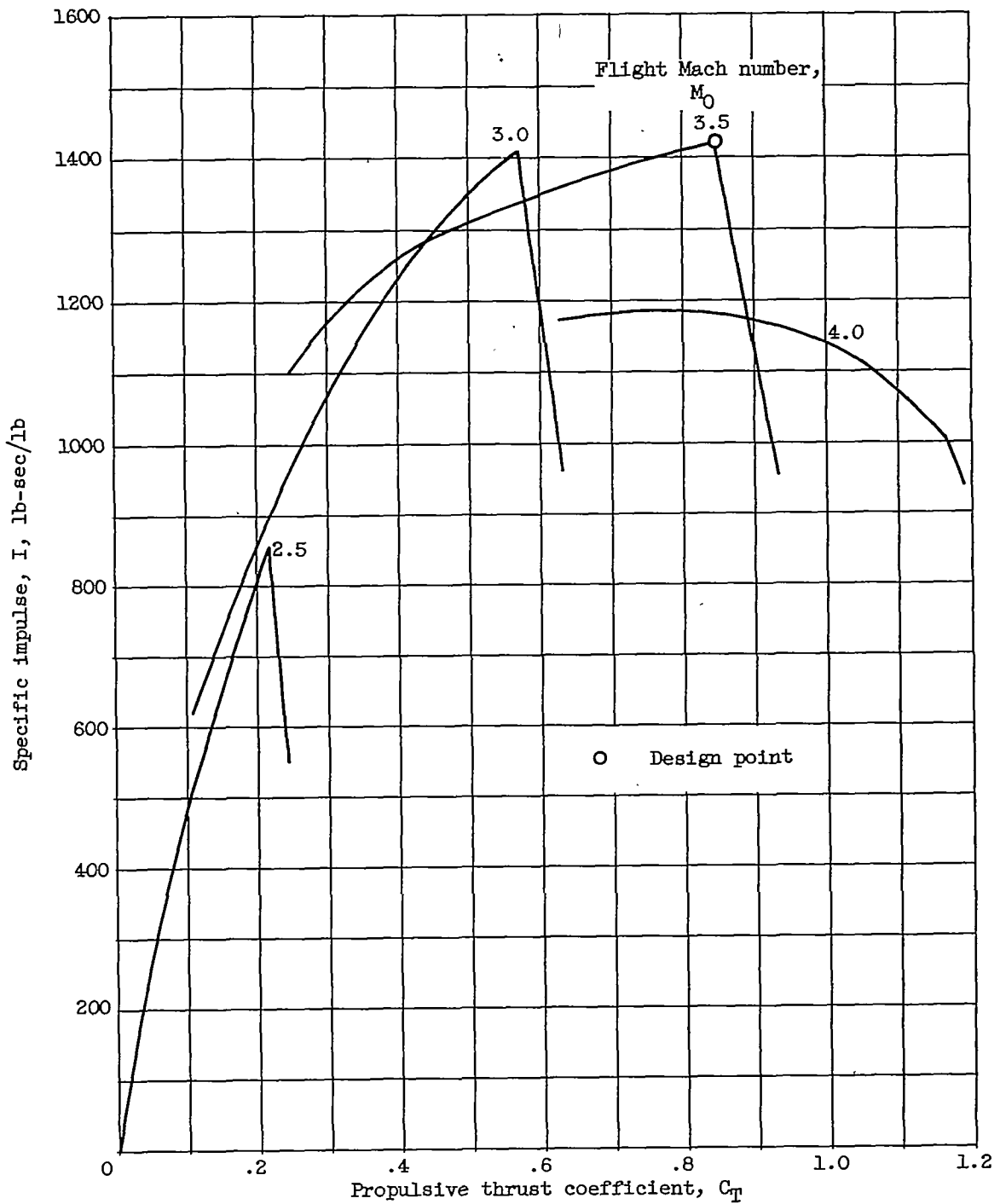


Figure 15. - Off-design performance of fixed-geometry ram-jet engine designed for flight Mach number of 3.5, combustion-chamber-inlet Mach number of 0.200, and engine total-temperature ratio of 2.25. Combustion efficiency, 0.87; ratio of specific heats for exhaust gases, 1.30.

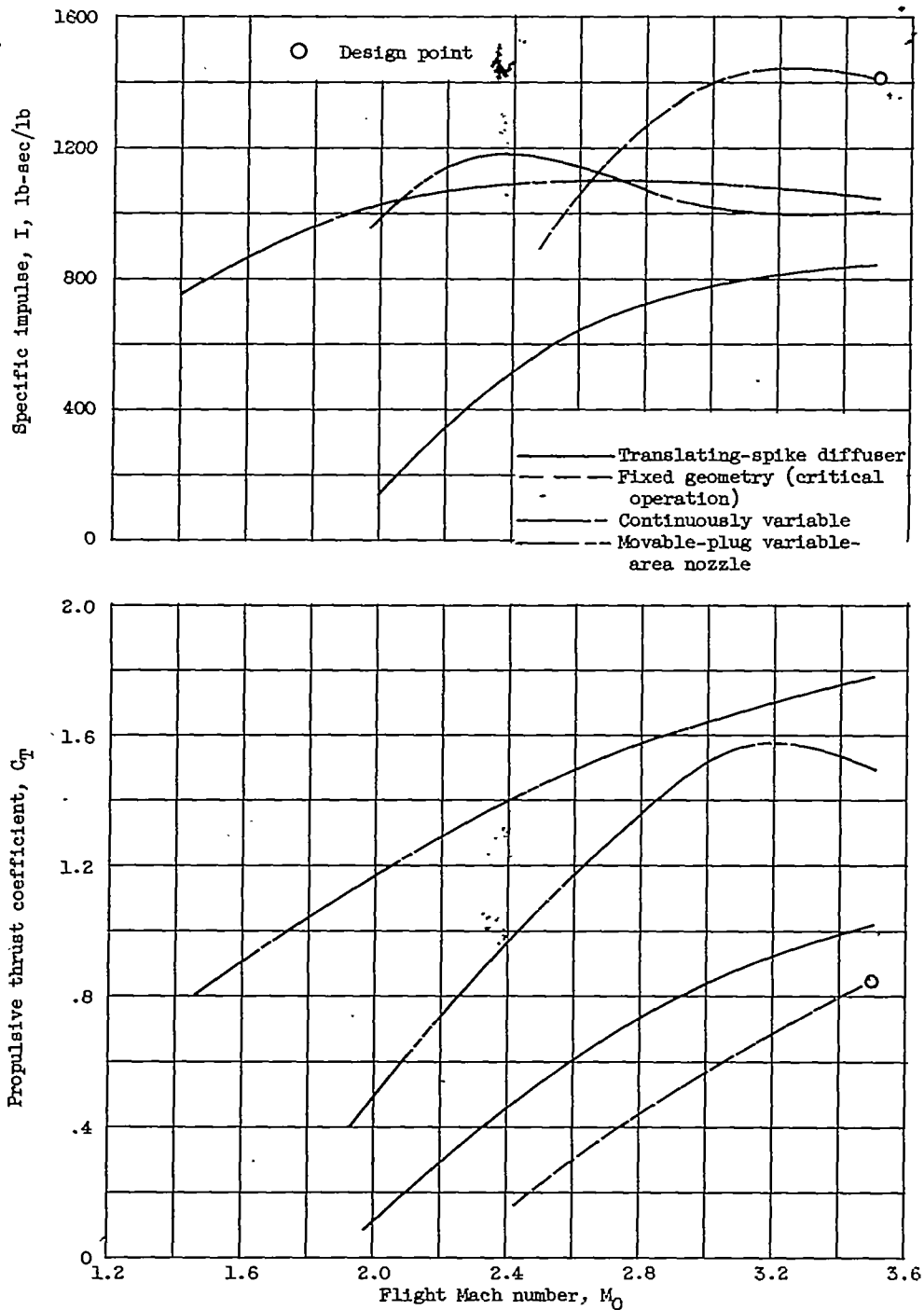


Figure 16. - Off-design performance of various fixed- and variable-geometry ram-jet engines operating at maximum thrust. Engines designed for flight Mach number of 3.5, combustion-chamber-inlet Mach number of 0.200, and engine total-temperature ratio of 2.50. Combustion efficiency, 0.87; ratio of specific heats for exhaust gases, 1.30.

~~CONFIDENTIAL~~